ADDIS ABABA UNIVERSITY

ADDIS ABABA INSTITUTE OF TECHNOLOGY

SCHOOL OF MECHANICAL AND INDUSTRIAL ENGINEERING

"Performance Analysis of Small-Scale Milk Pasteurization using Solar Thermal Energy"

A thesis submitted to School of Graduate Studies of Addis Ababa University as a partial fulfillment for the requirement of Masters of Science in Mechanical Engineering (Thermal Engineering)

By: Derese Degefa

Advisor:

Dr. Ing. Demiss Alemu

October, 2018

Addis Ababa, Ethiopia

ADDIS ABABA UNIVERSITY

ADDIS ABABA INSTITUTE OF TECHNOLOGY

SCHOOL OF MECHANICAL AND INDUSTRIAL ENGINEERING

This is to certify that the thesis is prepared by Derese Degefa, entitled: ***Performance Analysis of Small-Scale Milk Pasteurization Using Solar Thermal Energy*** and submitted in partial fulfillment of the requirements for the Degree of Master of Science in Thermal Engineering obeys with the regulations of the University and meets the accepted standards.

Submitted by:

Derese Degefa	_____	_____
Name	Date	Signature

Approved by Board of Examiners

Dr. Ing. Demiss Alemu		
Advisor	Date	Signature
Dr. Adbulkadir Aman		
Internal Examiner	Date	Signature
Dr. Ing. Wondossen Bogale		
External Examiner	Date	Signature
Dr. Yilma Taddese		
Chairman of SMIE	Date	Signature
Dr. Ermias Tesfaye		
Director of Post Graduate	Date	Signature

October 2018

Addis Ababa, Ethiopia

Declaration

I, the undersigned, declare that this thesis entitled "***Performance Analysis of Small Scale Milk Pasteurization using solar thermal energy*****"** is my original work under School of Mechanical and Industrial Engineering, AAiT, and has not been submitted by any other person for an award of a degree in this or any other University, and that all resources of materials used for this thesis have been duly acknowledged and a list of references is given.

Name:

Derese Degefa Jima _____

Signature

This thesis has been submitted to the Addis Ababa University with my approval as the University Advisor.

Advisor:

Dr. Ing. Demiss Alemu _____

Signature

TABLE OF CONTENTS

LIST OF TABLES

LIST OF FIGURES

LIST OF ACRONYMS

AAiT	Addis Ababa Institute of Technology
AgETSC	All-glass Evacuated Solar Tube Collector
EDGET	Enhancing Dairy Sector Growth in Ethiopia
DWC	Domestic Water Consumption
FAO	Food and Agriculture Organization
HTC	High-Temperature Collector
HTST	High Temperature Short Time
HX	Heat Exchanger
LMTD	Log Mean Temperature Difference
LTC	Low Temperature Collector
MATLAB	MATrix LABoratory
MTC	Medium Temperature Collector
Min	Minimum
Max	Maximum
Ref	Reference
SMIE	School of Mechanical and Industrial Engineering
SWHs	Solar Water Heating System
UHT	Ultra-High-Temperature
UP	Ultra-pasteurization
UpETSC	U-pipe Evacuated Tube Solar Collector
WGETSC	Water in glass Evacuated tube solar collector

NOMENCLATURE

Notations

H	Global solar radiation on a horizontal surface
Ho	Extraterrestrial solar radiation on a horizontal surface
S	Sunshine hour in day
Z	Elevation above sea level
$\emptyset$	Latitude
T_d	Sunshine duration
ω	Hour angle
ω_s	Sunset hour angle
δ	Declination angle
G_{sc}	Solar constant
K_T	Clearness index
ST	Solar Time
I_T	Total hourly solar radiation
θ_i	Angle of incidence
θ_z	Zenith Angle
β	Tilt angle
A_c	Collector gross area
T_a	Ambient temperature
T_g	Glass temperature
T_p	Absorber plate temperature
T_f	Fluid temperature
α	Absorptive coefficient
ε	Emissivity
σ	Stefan-Boltzmann constant
F_R	Collector heat removal factor
C_p	Heat capacity of water
U_L	Overall heat loss coefficient
τ	Glass transmittance
η_0	Collector optical efficiency
ΔT_{LMTD}	Average logarithmic temperature difference

U	Coil overall heat transfer coefficient
C_r	Coil heat loss coefficient
A_o	Coil heat transfer area
D_{st}	Milk storage inner diameter
D_c	Coil mean diameter
P	Coil pitch
N_{coil}	Number of coils turns
L_{coil}	Coil length
ε	Heat exchanger effectiveness
f	Friction factor
Re	Reynolds number

Units

hr.	Hour
m	Meter
mm	Millimeter
min	Minute
lt	Liter
K	Kalvin
^{0}C	Degree Celsius
Kg	Kilogram
Pa	Pascal
S	Second
W	Watt
Wh	Watt hour
KWh	Kilo Watt hour

ACKNOWLEDGMENTS

First and for most, I want to thank the Almighty God who is at my side and strengthened me throughout my career. Next, I would like to express my deepest thanks to my advisor Dr. Ing. Demiss Alemu for his guidance, intellectual support, invaluable advice throughout this thesis and suggestion to work on the title.

I am also thankful to Wollo University and Ethiopian Ministry of Education for financially supporting my MSc. Education in Addis Ababa University and National Metrology Agency. I am also grateful to Fikadu Geremu for his kind help, while writing a MATLAB program and Taye Meseret for his supportive ideas and data analysis.

Last but not least, I would like to thank my family and my classmate students for their unlimited support during my stay in Addis Ababa University and peoples who helped me to finish this work.

ABSTRACT

In this paper, milk pasteurization system was developed by utilizing solar energy for off grid peri urban milk producers of Kombolcha as having warm climate condition. While, milk is perishable foodstuff and easily spoilage but milk producers in area are not used any milk preservation system. Thus, this study aim to study performance analysis of solar energy of the location for small-scale milk pasteurization with coil heat exchanger fully immersed into the milk storage tank. The simulation of the studied model analysis was done with a MATLAB code and the performance of the milk pasteurization system was predicted.

The system uses 2.11 m^2 gross area of an Evacuated tube solar collector and the solar radiation intensity on inclined surface of the location obtained was about 480 W/m^2 to 920 W/m^2 with glass temperature of 25 ^0C to 36.2 ^0C. The average monthly useful energy gained by the collector was 780 Wh to 1500 Wh and the maximum hot water temperature exit from collector was between 80 ^0C to 83.42 ^0C using water as heat transfer fluid at the solar noon for each month of the year. After energy loss to the ambient, the hot water temperature in the thermal storage tank or inlet to the coil heat exchanger was about 69.0 ^0C to 78.2 ^0C. Moreover, the pasteurized milk temperature found to be 65.0 ^0C to 69.2^0C. Overall results indicate that, solar based milk pasteurization system was viable technology in this manner and it achieved the acceptable milk temperature range being heated to destroy microorganisms that leads milk spoilage.

Key words: MATLAB, Pasteurization, Coil heat exchanger, Thermal Storage

CHAPTER ONE

INTRODUCTION

1.1 Background

Milk is a nutritious food which consists of an important part of human's diet, that contribute for proper functioning of the body and relevant for maintaining good health during all ages and stages of life. It is consumed as fluid or it is used for the production of other dairy products such as butter, cheese, ice cream, etc. [1-2]. Milk and milk products are among the World's major food products, consumed by millions of people from all over the world on an everyday basis. According to FAO (Food and Agriculture Organization) in 2016 statistics study, the world total milk production forecasted was 816 million tons [3].

Taddesse, et al. [4] reviewed that, Ethiopia is one of the Sub-Saharan African developing countries with a large potential in livestock population, being first among African countries and ninth in the world. Estimates from farmer holding in rural areas indicate that the country has about 53.9 million cattle, 22 million goats, 26.0 million sheep and 2.3 million camels [5]. Cattle has the largest contribution (81.2%) of the total national annual milk output, followed by goats (7.9%), camels (6.3%) and sheep (4.6%), Despite its potential for dairy development, productivity of indigenous livestock genetic resources in general is low, and also the direct contribution it makes to the national economy was limited.

Consequently, Ethiopia has 10.5 million dairy cows which on average produce 1.5 liters of milk per day and the average annual milk consumption was 19 liters which is below the African average of 40 liters, contrasted with a worldwide consumption of 105 liters and the annual milk production growth rate is 1.2 percent which falls behind the annual human population growth of 3 percent estimated [5-6].

This is a great gap at the country level which result shortage of supply of dairy products and requires the country to spend hard currency to import dairy products from abroad and need expand of domestic dairy industries for milk producers will have to become more market-oriented [7-8]. However, there are a number of dairy processing firms, each produces to accommodate their own raw milk demand and they are unable to satisfy the majority of the consuming population through providing processed milk and dairy products in Ethiopia [9].

Moreover, milk and milk products are economically important farm commodities and dairy farming is an investment option for smallholder farmers. Because it, plays a very important role in feeding the rural and urban population of Ethiopia. Kassahun, et.al [10] recent study, in Kombolcha there are 32 different urban and peri urban around 5-10 km from center of town cattle

fastening association which holds 66 members were monitored and guided by Micro and Small Enterprise office. In peri-urban level livestock farmers' milk production account 60%, followed by 16.7% profit from income generation. However, the quality of milk production is poor due to liquid milk handled traditionally and have a very limited shelf-life.

Atia, et al. [11] pointed that, milk is a perishable foodstuff due to excellent medium for the growth of microorganisms which cause spoilage. For this reason, milk is heated to a specific temperature for a specific period of time, to killing harmful microorganisms for making safe milk and one of the best-known heat treatments in milk processing plant was pasteurization which is carried out between 60 - 75^0C according to the processor type to extend the shelf-life and to improve the quality and minimizing the risk of milk poisoning [12].

Modi, et al. [13] also explained that, thermal processing is an essential step in milk production process adopted by the dairy industry. In producing fluid milk and milk products through applying thermal treatments such as heating and cooling requires significant amount of energy. However, energy consumption is a crucial issue in dairy industry for both economic and environmental point of view.

Patel, et.al [14] reviewed that, solar panel or concentrator-based milk pasteurizer system in dairy industry able to meet the demand of pasteurization. It was observed that base temperature of solar heated water reached up to 100˚C and pasteurizer has easily attained pasteurization temperature ranging from 65 to 75˚C in two-three hours.

However, among some part of rural and urban areas of Ethiopia, Kombolcha was one of an efficient solar energy potential found in South Wollo Zone of the Amhara Regional State of Ethiopia. And Ethiopia, still suffer reliable, effective and sufficient electricity in many parts of the country, in particular rural and other off-grid areas are suffering the most.

Thus, the aim of this thesis was to study performance analysis of the solar energy potential of the location for small scale milk pasteurization for off grid peri urban milk producers in Kombolcha, which are the predominant milk producers in the area.

1.2 Statement of Problem

Consumption of raw milk and milk products such as cheese, cream, butter and yoghurt are commonly consumed in sub-Saharan Africa including Ethiopia [15]. However, the national average capita consumption of milk in Ethiopia is 19 kg as compared to 27 Kg for other African countries and 100 kg to the world per capita consumption [5]. In Ethiopia, moreover, production and consumption of raw milk and various dairy products often takes place under unsatisfactory hygiene conditions mainly due to inadequate dairy infrastructure such as refrigeration facility,

absence of clean water and limited knowledge of handling of milk and milk products [16] Furthermore, critical distribution elements such as milk collection, chilling and transportation are not well organized in Ethiopia dairy production and market systems are typical constraints which leads to lower economies of the country from the resource. Consequently, transaction costs are high, and up to 20 - 35% of milk is spoiled or otherwise lost [6].

Makita, et.al [17] identified that, consumption of dairy products was high and microbial are the common causes of foodborne illnesses in many parts of the world and harmful for the human health. Even, a raw milk from healthy cow may contain a low microbial load, but the microbe may increase, multiply if it stored at normal temperature of atmospheric environment [18].

However, according to Yilma, et.al [19] reviewed from earlier research conducted in Ethiopia revealed that, the microbial counts of milk and milk products produced and marketed in the country are generally much higher than the acceptable limits.

Flores-Flores, et.al [20] suggested, it is very important that milk is free of toxic compounds that can be harmful for humans, especially for children which are more susceptible to the action of toxic compounds, because they are the largest consumers of milk as it is one of the principal foods during their first years of life.

To increase the quantity and quality of milk and milk products being offered to consumers and to increase development of the dairy sector in Ethiopia, small-scale livestock enterprises milk producers in different urban, peri-urban and rural areas now a time contributes immensely to poverty mitigation and improve nutrition in the country [5].

However, per urban milk producers (about 80 to 230 liters per day) in Kombolcha off grid areas have a serious problem of milk preservation facility and getting their milk to market. This is especially due to liquid milk handled traditionally and have a very limited shelf-life. Because, unpasteurized milk spoils easily and there is also no a nearby milk dairy processing facility as well.

Thus, this research study was aim to utilize solar energy for milk pasteurization process. Since, to keep the quality of raw milk and to increase its shelf life is a vital issue for human health as well as to increase its business sector for economic growth and food security of the country.

1.3 Objective

1.3.1 Main objective

- The main objective of this thesis was, to study performance analysis of small-scale milk pasteurization using solar thermal energy for hundred -liter milk per day.

1.3.2 Specific objective

Specific objectives were to:

- Collect weather data and estimating solar energy potential of the location.
- Model design a solar thermal collector, sizing helical coil heat exchanger and milk storage tank
- Utilize MATLAB code simulation for performance analysis of the overall modelled milk pasteurizer under transient condition.

1.4 Scope of the study

The scope of this study was from solar energy potential estimation of the study location to a solar milk pasteurizer system performance analysis through developing a MATLAB code.

In the milk pasteurization system considered (Fig 3.3), the main components are evacuated tube solar collector, thermal storage tank, coil heat exchanger and the milk storage tank. For this component a transient governing equation was developed to study the hourly useful heat gained by the collector, the hot water temperature exits from the collector and the hot water temperature in thermal storage tank. In addition, coil HX and milk storage tank sizing as well as pumping power requirements for circulating pump are done. Finally, the performance analysis of pasteurized milk temperature was studied. However, the cost analysis, testing & installing of the considered system was not performed.

1.5 Significance of the study

This study come up with a number of significances.

- A significant benefit of this research was, the utilization of solar energy for milk pasteurization and to provide diary processing facilities for small – scale milk producers.
- To create awareness for other milk producer areas, which have solar energy potential to adopt such technologies
- To increase domestic dairy sector involvement through having a raw milk collection center at different dairy farming areas.
- To reduce Ethiopia dairy sector constraints and hard currency the county spends to import dairy products from abroad.

1.6 Thesis Organization

This thesis organized into six chapters. This is the first chapter gives the details about the studies introduction with elaborating the problems. In addition, it also lays down the objectives of the thesis and its relevance.

Chapter 2 introduces, previous research studies related to solar energy utilization, milk pasteurization processes, solar water heating system and other necessary background information for the current study.

Chapter 3 presents, the methodologies and detail mathematical model design of solar thermal collector for MATLAB coding.

Chapter 4 deals with sizing the coil heat exchanger parameters and calculation of the total pressure drop in the system and pumping power requirement.

Chapter 5 present the result and discusses the graphically generated outputs from model simulations. Chapter 6 provides the conclusion and recommendation for future works.

CHAPTER TWO

LITERATURE REVIEW

2.1 Introduction

As mentioned in Chapter 1, milk production capacity of Ethiopia in liters of milk per day produced and average annual milk consumption relative to Africa and the world, research gaps and basic milk preservation constraints were introduced. However, in this chapter from previous research studies related to solar milk pasteurization system model design, operation, performance analysis and material selection are reviewed to provide background for the current study and important and key terms are also defined and explained.

2.2 Overview of Ethiopia's Dairy Sector Constraints

Tadesse, et.al. [4] explained that, dairy production system is a biological efficient system that converts large quantities of cellulose from livestock, which is milk, the most nutritious food to man. Dairy production is a critical issue in Ethiopia, a livestock-based society where livestock and its products are more important sources of food and income. However, dairying has not been fully exploited and promoted.

Desissu, [21] identified that, there are four major milk production system in Ethiopia dairy farming based on climate, landholding and farming systems. These are the pastoral dairy production system, highland smallholder's dairy production system, urban and peri-urban (small and medium dairy farms in backyards in and around towns and cities) dairy production system.

From this production system, rural smallholders produces about 63% and small urban or peri-urban producers about 22% contributes to the national milk production capacity of the country. However, the pastoral system mainly practiced in the lowlands, in this system, milk production per unit area is low and highly seasonal and three-fourth of the milk produced by rural households is consumed at home [5].

Urban dairy systems in general are located in cities and/or towns and focuses on production and sale of fluid milk. Peri-urban dairy production system is mainly operating in areas where the population density is high such as around big cities and smaller towns. In this system, it is estimated that 71% of the producers sell their milk directly to consumers and it is an important system safeguarding the large milk demand-supply variance in Ethiopia.

This market-oriented smallholder urban and peri-urban dairy production systems have immensely contributing towards filling in the large demand –supply gap of fluid milk and milk products in urban centers, where consumption of milk and milk product is remarkably high [7].

However, there are major dairy sector constraints which hinder the milk production capacity of Ethiopia in spite of enormous livestock resource as reviewed and studied by some researcher.

The critical distribution elements such as milk collection center, chilling or refrigeration facility and transportation, access to services and inputs, inefficient and inadequate milk processing technologies, marketing and absence of clear policy support to the sector the absence of clean water and limited knowledge of the clean handling of milk and milk products are also identified as major constraints that hinder dairy sector development in the country [6-8].

In addition, dairy industry in the country are also constrained by several technical and economic factors and the national milk production remains among the lowest in the world, even by African standards [16].

According to Yilma, et.al [19] reviewed, there is a research gap and the weak linkages among the different actors in the dairy value chain (Fig: 2.1) are some of the important factors that contribute to poor development in Ethiopia's dairy sector as well.

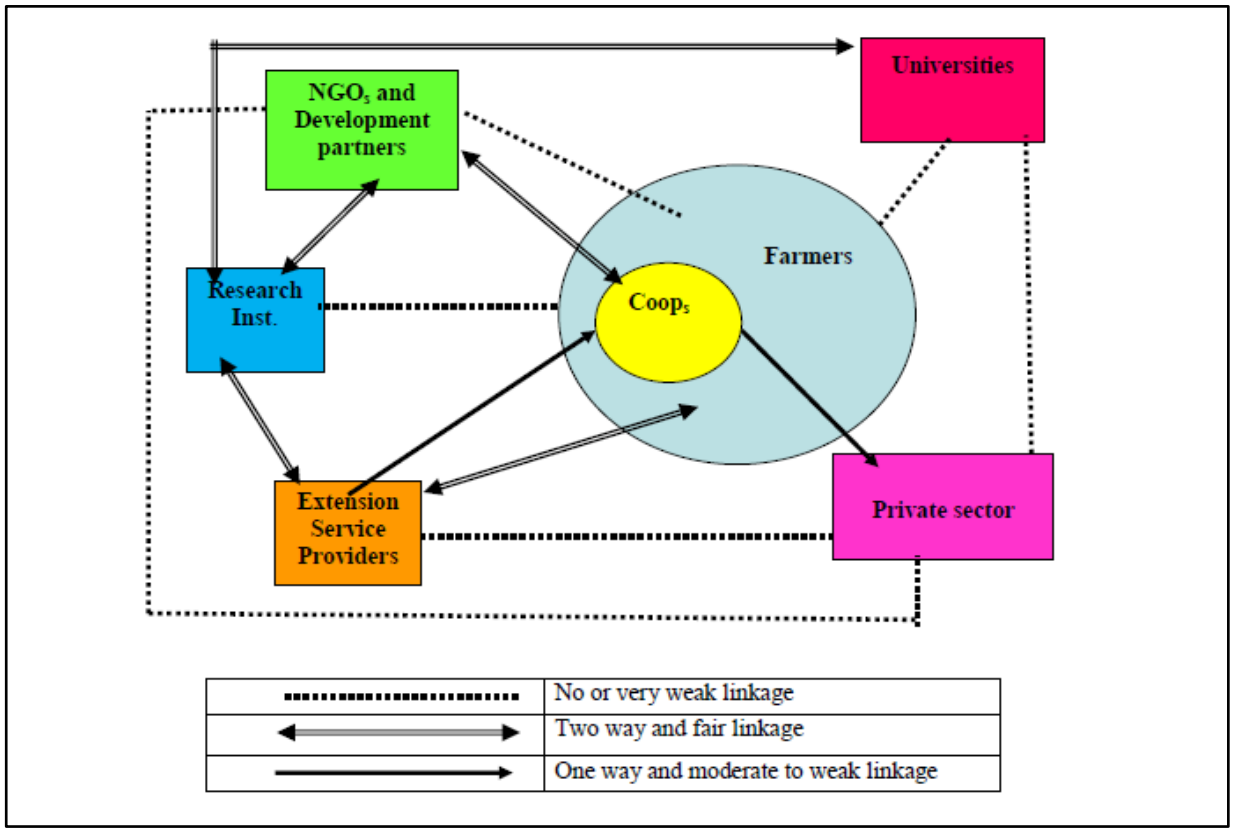

Figure 2.1: Linkages among the various actors in the Ethiopian dairy value chain [19]

2.3 Pasteurization Process

Karunasree, [22] reviewed, pasteurization is a heat treatment process, which is used to inactivate pathogenic and spoilage microorganisms in milk and other products at low temperature. However, it is common for milk pasteurizing and normally carried out in hot water or steam heating systems

using batch or continuous flow pasteurization systems. It was invented by French scientist Louis Pasteur during the nineteenth century [23].

In general, there are two types of milk pasteurization processes. The first was batch or vat pasteurization process, if consist a tank which filled with the milk, heated to the desired temperature, and held for the specified time before cooling. The second was a continuous types of pasteurization process it uses effective heat exchangers to heat and cool the liquid food.

Patel, et.al [14] stated that, renewable solar energy utilizing in dairy by using solar panels or concentrator-based milk pasteurizer system is developed to meet the demand of pasteurization. It was observed that base temperature of solar heated water reached up to 100˚C and pasteurizer has easily attained pasteurization temperature ranging from 65-75˚C in two-three hours.

In this thermal treatment, heat exchangers are used for heating and cooling the food product, while the target micro-organism or enzyme is inactivated at high temperature for a given residence time in a holding tube.

Yildirim, et.al [12] explained that, in milk processing plant, pasteurization is one of the best-known heat treatment process. In this process, heat transfer is specially provided by hot water using different types of energy sources such as natural gas, coal, electricity, renewable energies, etc.

They also informed that, cooling is accomplished by conventional vapor absorption systems with their lower initial and operating costs compared to a cooling tower. However, the refrigerants (chlorofluorocarbons) used in the conventional systems are not environmentally friendly.

2.3.1 Purpose of Pasteurization

- To make milk safe for human consumption by destroying the pathogenic organisms, which may be present in milk, such as viruses, bacteria, protozoa, molds and yeasts.
- To improve milk preservation quality by destroying almost all spoilage microorganisms and enzymes that contributes to reduce the quality and the shelf-life of milk.
- Helps to retain good flavor over a longer period of time.

As noted in Ref [13] pasteurized milk is expected to have a shelf life of 14 to 20 days. However, the shelf life of pasteurized milk stored at ambient temperature depends upon the efficiency of the pasteurization process.

2.3.2 Types of Milk Pasteurization

Simran, [23] identified, there are four common types of milk pasteurization that vary with temperature and time the milk is held at that temperature.

- Batch or Vat Pasteurization
- High Temperature Short Time (HTST)
- Ultra-High-Temperature (UHT)
- Ultra-pasteurization (UP)

Table 2.1: Temperature-time pasteurization requirements for fluid milk

Pasteurization Types	Time	Temperature
Batch/ Vat Pasteurization	30 minutes	63^0C
High temperature short time Pasteurization (HTST)	15 seconds	72^0C
Higher- Heat Shorter Time (HHST)	1.0 second	89^0C
"	0.5 seconds	90^0C
"	0.1 seconds	94^0C
"	0.05 seconds	96^0C
"	0.01 seconds	100^0C
Ultra-Pasteurization (UP)	2.0 seconds	138^0C

2.4 Solar Thermal Energy

Farjana, et.al [24] reviewed in simple words solar thermal energy is the energy that we get from heat conversion gained from solar irradiation and termed as solar thermal energy. Like other renewable energy systems, solar thermal energy can replace the fossil fuels in industrial systems.

This solar source of energy is sustainable, it does not provide any greenhouse gas emissions and environmentally friendly sources of energy. It is free and maintainable as the sun is here to stay. Jamar, et.al [25] reviewed that, solar water heating system is an effective technology for converting solar energy into thermal energy. The efficiency of solar thermal conversion is around 70% when compared to the solar electricity direct conversion system 17%.

In commercial or industrial plants, this energy conversion system employs a variety of solar thermal collectors along with concentrators which accumulate and deliver solar radiation are used for heat generation process. The type of solar collector, working fluids, installation parameters, heat exchanger specifications need to be considered for the specific process operation [24].

In general, solar thermal energy applications, for water heating are accomplished through solar collectors and these devices are responsible for the capture of solar radiation and transferring the thermal energy to a fluid [26].

2.5 Solar Water Heating System

Fathima, et. al [27] explained that, solar water heating systems, which use the sun's energy rather than electricity or gas to heat water, can efficiently serve up to 80% of hot water needs with no fuel cost or pollution and with minimal operation and maintenance expense.

Sadhishkumar, et.al [28] reviews that, solar water heating is one of the popular passive systems for providing hot water for small-scale applications and widely used all over the world due to its simplicity, technological feasibility, economical and commercial viability. This system has a potential to reduce 60–80% of thermal energy to provide heated water over a year.

Deepak, et al. [29] stated that SWHs is the process of providing hot water with the help of solar energy. In all plants in which milk treatment requires raising the temperature of milk, hot water is used as the heating medium in both domestic and industrial sector applications. They are considered as the most cost-effective alternatives among all the solar thermal technologies currently available.

Patel, et. al [14] explained that, the solar heated water temperature reached up to 100˚C through absorbing solar energy, which was used successfully for attained pasteurization temperature ranging from 65-75˚C. However, the amount of hot water produced from SWHs critically depends climatic parameters such as solar radiation, ambient temperature and wind speed.

This solar water heating system consists of several basic components such as; the solar collector panel, thermal storage tank and heat transfer fluid, circulating pump (necessary in active system), auxiliary heating unit, piping units and heat exchanger [25]. This total system was called solar water heating system. It works on the basis of the density inequality of hot and cold water or thermosiphon [29].

2.5.1 Types of Solar Water Heating System

Wang, et.al [30] reviewed that, a solar water heating system can be categorized into direct and indirect systems based on whether or not they require a heat exchanger. In a direct system, the service water is directly circulated between the water tank and the collect, while for an indirect system, a heat transfer fluid, usually anti freezer, distilled water or organic fluid is circulated through the solar collector. A heat exchanger is employed to affect the heat transfer from the collector to the service water in the tank.

They also informed that, the heat exchanger could be used inside or outside the hot water tank and the indirect system in most situations performs better than the direct one, which is less climate-selective and more suitable for use in regions that experience cold temperatures.

Jamar, et.al [25] stated that, in general solar water heating systems classified into two as shown in Figure 2.2. The active system consists of the direct flow (open loop) system and indirect flow (closed loop) system; whereas the passive system contains thermosiphon and integrated collector storage.

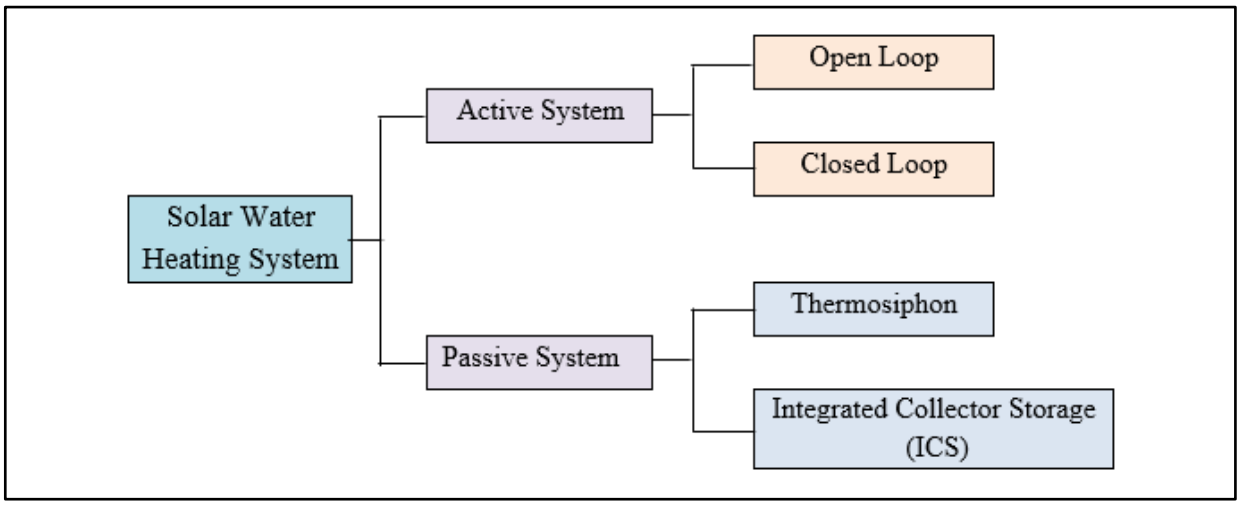

Figure 2.2: Types of Solar Water Heating System [25]

2.5.2 Active Solar Water Heating Systems

Wang, et.al [30] defined that, active water heating system is the one uses electrical pumps to transfer thermal energy, valves and controllers to circulate water or other heat transfer fluids through the collectors. This system is also known as forced circulation system and it can be an open loop (direct) active system or a closed loop (indirect) active system [25].

Open loop (direct) active system heats the actual household water in the solar collectors. Once heated, the water is pumped into a storage tank and then piped to spout for use at home. Whereas closed loop (indirect) active system uses heat to transfer fluids that are usually a water-antifreeze mixture.

After heat-transfer fluid was heated in the solar collectors, it was pumped into a storage tank where a heat-exchanger transfers the heat from the fluid to the raw water. This system has an advantage over passive system, in the range of 30 – 50% its efficiency is usually between 35% and 80% [30].

2.5.3 Passive Solar Water Heating System

Jamar, et.al [25] stated that, the passive system utilized natural convection heat transfer due to density differences. This system is based on a simple mechanism, where the heated fluid loses density and becomes lighter and thus flows up toward the collector and then into the storage tank, while the cold fluid flows down toward the tank floor and enters the collector without using mechanical devices [30].

There are two basic types of passive systems:

- **Thermosiphon systems:** In this system, water flows through the collector and the warm water rises as cooler water sinks. The collector must be installed below the storage tank so that the warm water will rise into the tank as shown in the Fig 2.3.
- **Integrated collector storage:** This system integrates, the solar collector and the thermal storage tank components function as a single unit. It is the simplest forms of solar water heater on the market and becoming a very popular choice of solar water heater, it also reduced the cost, as they integrate the collector and the thermal storage tank in the same construction [25].

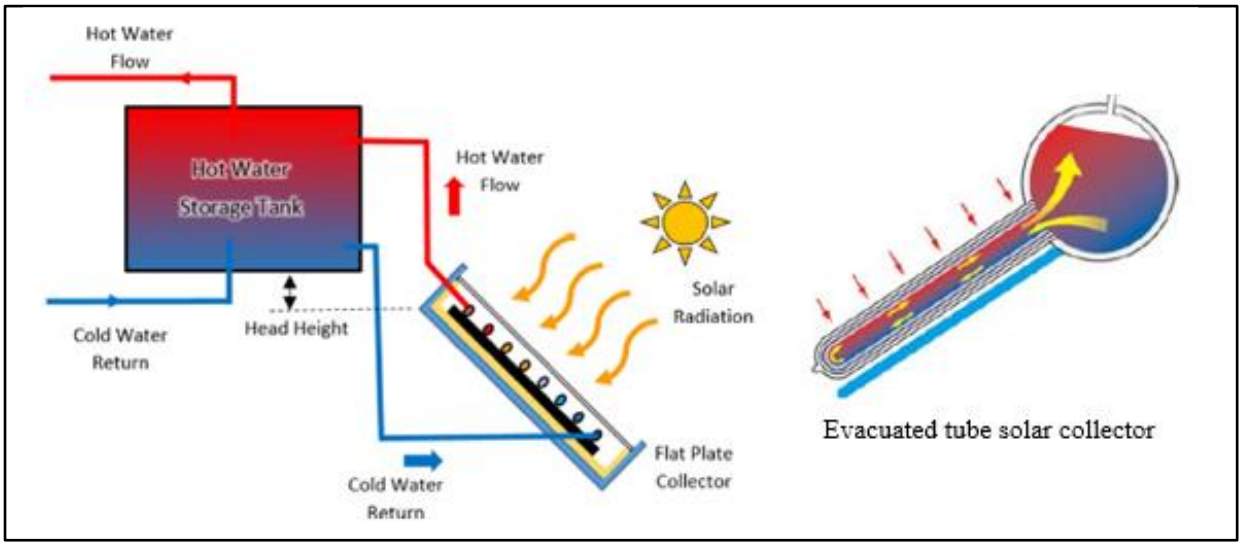

Figure 2.3: Thermosiphon principle [25]

2.6 Solar Thermal Collectors

Solar thermal collectors are a special kind of heat exchangers that convert solar radiation into thermal energy through a transport medium or a heat transfer fluid (HTF) [11]. Currently, two types of solar collectors namely flat plate and evacuated tube solar collectors are commonly used in a solar water heating system [31-32].

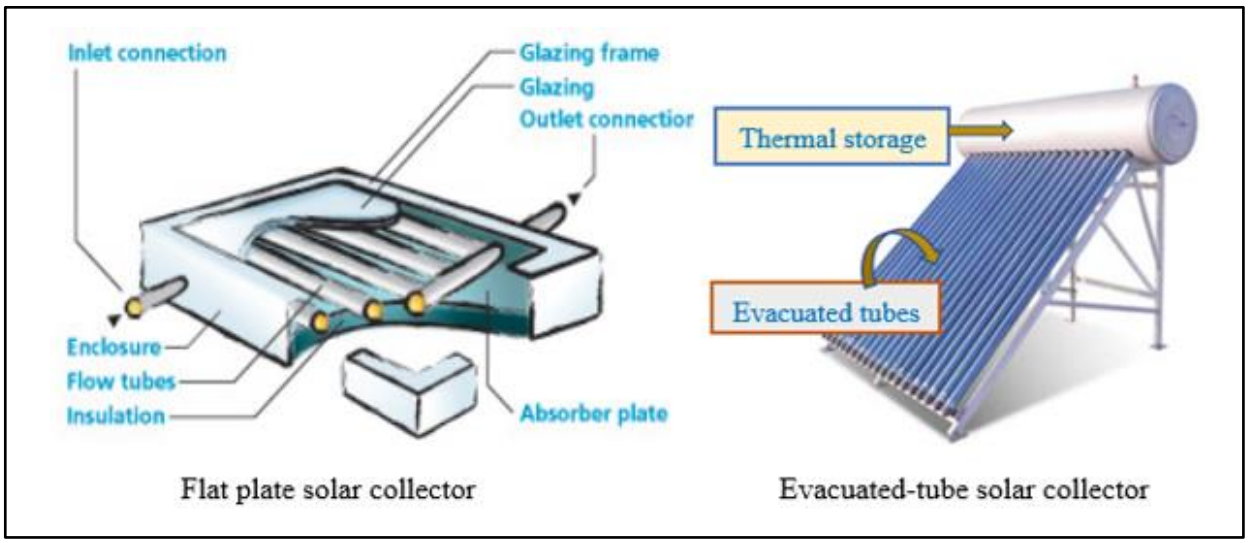

Figure 2.4: Types of Solar Thermal Collectors [31]

2.6.1 Flat-plate solar collector

A flat-plate collector (FPC) is the heart of a SWH system. However, operate efficiently at low temperatures, which limits their applications for domestic water heating and space heating [31].

It consists of a selectively coated a flat-plate absorber plate, a transparent cover to reduce top heat-losses from the absorber plate, heat-transport fluid to remove heat from the absorber plate, tubes/passages for the flow of the HTF, a heat insulating support to reduce heat loss from the collector, and a protective casing to ensure the components are free from dust and moisture.

Fathima, et.al [27] stated that, the conventional flat plate collectors are suited for warmer climates and for the times when the intensity of the solar radiation is substantially high. In addition, their benefits are reduced when they are exposed to cold, cloudy and windy days. Furthermore, when exposed to weathering conditions, the tubes and the insulation tend to deteriorate thereby causing loss of performance.

2.6.2 Evacuated-tube solar collector

Sabiha, et.al [33] explained that, ETSC is used to capture solar radiation, which is then turned to thermal energy and transferred to a working fluid. It is made of parallel evacuated glass pipes. Each evacuated pipe consisting of two tubes, one is inner and other is outer tube.

Yadav, et.al [34] stated that, these two glass tubes are made from extremely strong borosilicate glass. The outer tube is transparent allowing light rays to pass through with minimal reflection and the inner tube is coated with a special selective coating (Al-Nickel/Al) which features excellent solar radiation absorption and minimum reflective characteristics.

However, the two tubes are fused together on top to create a vacuum and the existing air is pumped out. This allows the heat stays inside the inner pipes and collects solar radiation efficiently and this makes an ETSC is the most efficient solar thermal collector. Researchers in Ref. [33] reviewed that, evacuated tube collectors are subdivided into two main types. The first type is the single walled glass evacuated tube and the other type is the Dewar tube type which consists of inner and outer glass tubes separated by vacuum space as shown in Fig 2.6.

According Aboulmagd, et.al [35], the first type is the direct flow collector where the heat transfer liquid is pumped into the tubes whereas the second type consists of heat pipes inside vacuum sealed glass tubes. However, there are many variations of the two basic types; for instance, heat extraction can be through a U-pipe, heat pipe or direct liquid contact [33].

Water in glass Evacuated tube solar collector (WGETSC) or all-glass evacuated solar tube collector (AgETSC) is a direct liquid contact type and now in China widely used for sanitary water

heating, because of its low price and excellent low heat loss features [31]. According to Gao, et.al [36] stated that, the U-pipe Evacuated tube solar collector (UpETSC) was developed based on improving the WGETSC. A U-pipe (generally copper piping with diameter 8–10 mm) and aluminum fins are inserted in the interior cavity of the tube.

Fluid flows in the U-pipe to absorb and carry away the useful energy. Obviously, the key difference is that each evacuated-tube of a WGETSC is filled with working fluid but the fluid is only contained in the U-pipe of a UpETSC.

Gao, et.al [31] also informed that, the advantages of UpETSC lay in the tube attaining higher temperatures, longer service life and the ability to bear more intense pressure than those of the water in glass collector. The UpETSC has well-developed type of collector and rapidly expanded in the market even the costs are higher than the water in glass collector types.

Sabiha, et.al [33] reviewed from experimental works, the U pipe evacuated collectors have 25–35% higher energy storage capacity than water in glass. In addition, the energy storage and also pump operations are influenced by the flow rate and fluid thermal mass.

However, heat pipe is a thermal energy absorbing and transferring system with no moving parts which can transfer more energy than copper, where the heat pipes are the best-known conductor and can operate with a temperature up to 300^0C with 50% to 60% efficiency [37].

Jafarkazemi, et.al [38] identified from the experimental comparison between flat plate and heat pipe evacuated solar collector at similar weather condition within one year. The flat plate and evacuated collector generated 496 kWh/m^2 and 681 kWh/m^2 energies per unit area, respectively. Also, annual averages of thermal efficiencies were 46.1% and 60.7%, respectively.

ETSC is strong and long lasting if any tube is broken, it is just replaced, which is considered as a cheaper option as compared to a flat plate collector (FPC) which require the replacement of the whole collector. [32]

2.6.3 Working principle of U pipe Evacuated Tube Solar Collector

Fig: 2.6 illustrates a schematic diagram of the glass evacuated tube solar collector with U-tube and its cross-section view, adapted from [32]. As explained in Ref [35] [32], evacuated tube collector receiver consists of a copper U-tube inside a glass vacuumed tube, copper tube surrounded by a cylindrical aluminum fin pressed on it, which has the role of enhancing the heat transfer area between the inner glass absorber surface and the U-tube. Fluid flow in the collector is also represented in Fig. 2.5 [35].

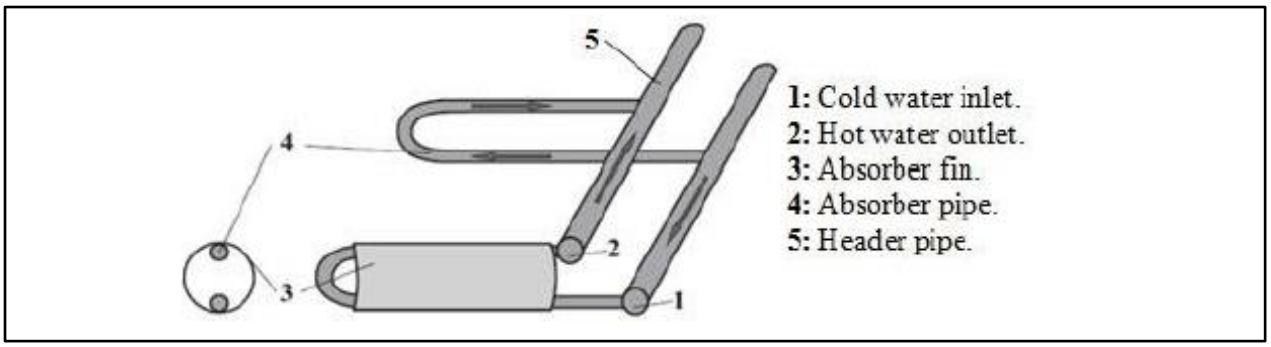

Figure 2.5: Fluid flow in the collector tubes [35]

As shown in Fig: 2.5 the working fluid (heat transfer fluid) enters the collector inlet pipe, then it is evenly distributed to the U-tubes, absorbs heat and, at the end, it is returned to the outlet header pipe. The outer cylindrical glass transmits the rays to the inner glass tube, which conducts the energy to the absorber fin. The energy transformed into heat is conducted by the fin to the copper U-tube and finally absorbed by the working fluid.

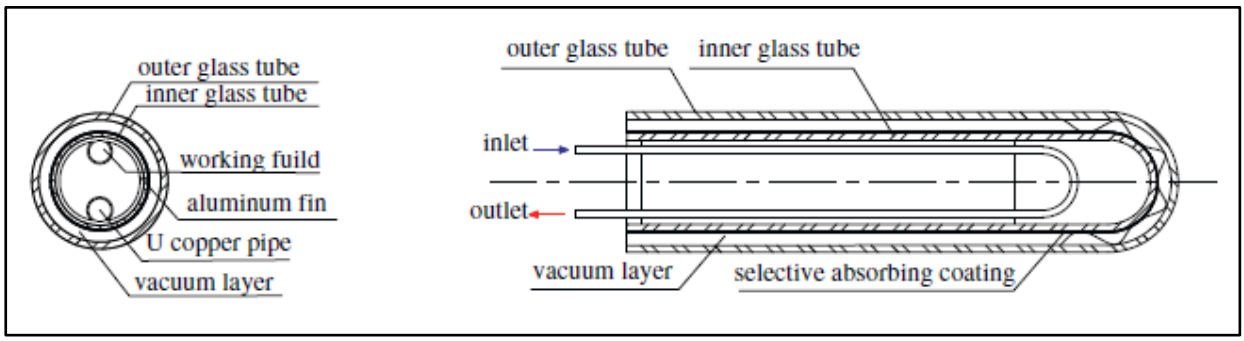

Figure 2.6: Schematic diagram of the glass evacuated tube solar collector with U- pipe tube [32]

Furthermore, Sabiha, et.al [33] also reviewed from many researcher's investigation, an Evacuated tube solar collector is more preferable than Flat plate collector due to some the following details.

ETSCs have much higher efficiencies than FPCs and collect both direct and diffuse radiations, also suitable for unfavorable climate. In contrast, FPC is mainly designed for sunny and warm climates because moisture and condensation cause early erosion of internal material which might cause system failure.

The peak energy output by FPC is gained only at midday when the sun is perpendicular to the surface of the collector, whereas the evacuated solar tube area able to track the sun passively throughout the day as for the cylindrical shape of evacuated tubes. This average output energy from ETSC over an entire year is 25 – 40% higher than FPC per net m^2.

2.7 Solar Collectors Selection parameter

According to Jamar, et.al [25] there are some considerations that must be employed in choosing the right solar collector in terms of heating requirements, the environmental conditions, the

collecting characteristics, the way the collectors are mounted (static or adjustable to follow the tracking of the solar radiation), tilt angle and the types of heat transfer fluid (water, water ethylene glycol solution and air).

Solar collecting characteristic can be non-concentrating collectors and concentrating collectors. For non-concentrating, it can be a flat type that has no medium to concentrate the incoming solar radiation, while for concentrating, it has reflectors to concentrate the energy falling on the aperture onto a heat exchanger with a surface area that is smaller than the aperture.

Suresh, et.al [39] suggest selection of solar collectors depend on several parameters, such as:

- **Operating temperature**

  As the thermal processes required solar collectors categorized as low temperature collectors (LTCs), medium- (MTCs) and high-temperature collectors (HTCs) with operating temperatures of < 80^0C, 80^0C - 250^0C, and >250 ^{0}C, respectively. LTCs are mainly used for water heating and space heating applications.

  MTCs are used for generating hot water, steam and hot air in industrial process heating and cooling applications, whereas an HTC is mainly used for power generation and for supplying hot water/steam.
- **Sun tracking position:** most of the LTCs and MTCs are stationary-type collectors and they do not track the sun, whereas HTCs are moving-type collectors and track the position of the sun over a day.
- **Cost or capital investment:** FPCs and Evacuated Tube Collectors (ETCs) are economical to generate heat up to 150 ^{0}C for process heating. While, HTCs (dish collectors) can generate heat greater than 150 ^{0}C but require high capital investment.
- **Life time:**

  ETC-type collectors are made of glass and are fragile in nature, whereas FPCs contain metallic components and have longer lives. In general, plant life for an FPC, an ETC and a Dish are 20,15 and 25 years, respectively.

2.8 Heat Exchanger

Heat exchanger is an essential device designed for exchanging heat between two or more fluids with different temperatures. They can be also classified in a number of ways, depending on their construction or on how the fluids move relative to each other through the device.

Panchal, et.al [40] reviewed that, heat exchangers are many in types and used widely in industries as well as in domestic applications due to increment in heat transfer applications now a days. They also identified that, shell and tube-type HEs are widely used in dairy and food industries.

However, under conditions of laminar flow or low flow rates, where a shell-and – tube heat exchanger would become uneconomical because of the resulting low heat-transfer coefficients.

Vishvakarma, et.al [41] and [42] reviewed that, the helical coils of circular cross section have been used extensively in food processing and preservation, dairy, refrigeration, storage tanks, heat recovery systems, power generation, air conditioning, etc.

Purandare, et.al [43] stated that, helical coil heat exchanger is superior to straight tubes in the heat transfer application due to the secondary flow developed in the curvature of the tubes and the centrifugal force observed in the fluid flowing which enhances the heat transfer in the coiled tube heat exchanger. Further, from experimental results the smaller coil and tube diameter the intensity of secondaries developed is higher. This increase in intensity of secondaries allows proper mixing of the fluid, which enhances heat transfer coefficient for the same flow rate. In contrast, increase in tube and coil diameter reduces the secondaries developed which reduces heat transfer coefficient [43].

In addition, it is well known that helical pipes provide enhanced inner convection heat transfer when compared to straight pipes and Fig: 2.7 shows the effectiveness of the helical coil heat exchanger is found to be also higher when compared to that of the straight tube heat exchange for all the inlet temperatures [41].

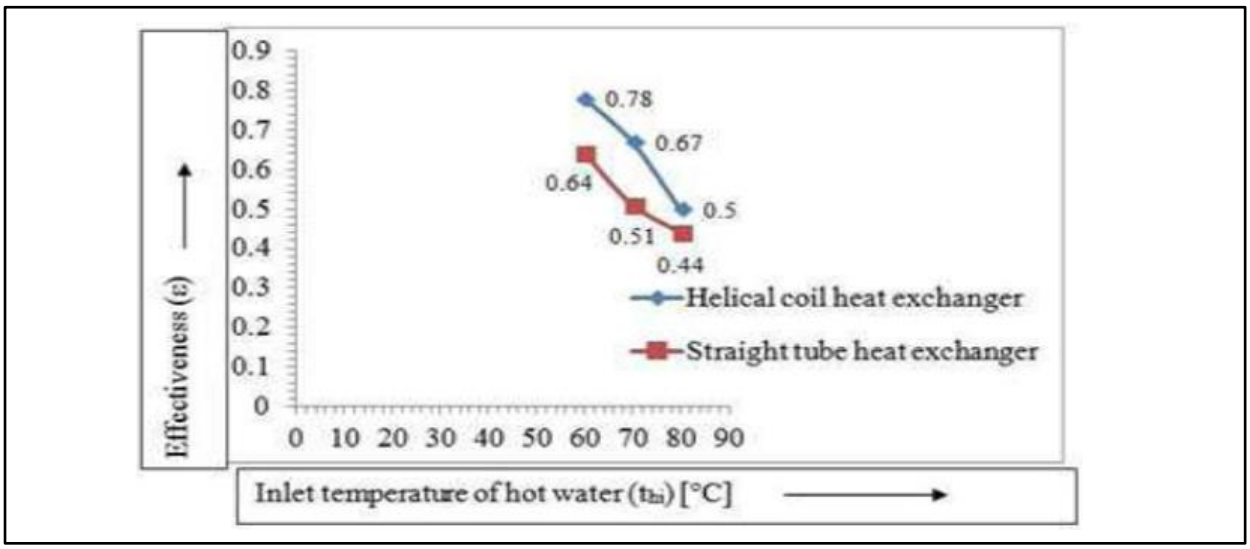

Figure 2.7: Variation of heat exchanger effectiveness with inlet temperature of hot water [41]

Huang, et.al [44] stated that, plate heat exchangers are widely used to pasteurize liquid food products like milk. However, the accumulation of fouling material on the heat exchanger plates shortens run time, reduces operating efficiency and may increase the risk of microbial contamination.

Shuhong, et.al [45] investigated experimental study, on the influence of the position of coil heat exchanger in SWHs thermal performance. From efficiency analysis the maximum annual solar

fraction and maximum collector efficiency are 42.2% and 31.4%, when the coil HX at the bottom of the tank as shown in Figure 2.8. And, they concluded that from experimental and annual simulation for long-term performance of SWHs it's better to have the heat exchanger at the bottom of hot water tank [45].

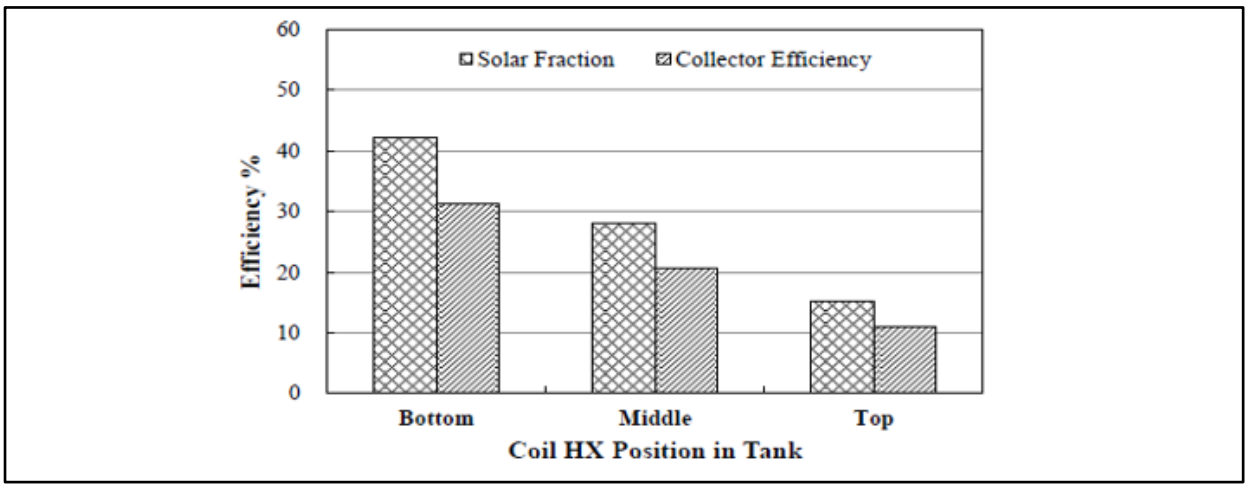

Figure 2.8: The solar fraction and collector efficiency of SWHs [45]

Fernández-Seara, et.al [46] carried out the same type of investigation as [45] considering two experimental set up with the coil placed at the bottom and top of the tank. Finally, they concluded that coil placed as near as possible to the bottom of the tank increase its storage capacity.

Basically, as reviewed by many researchers heat exchangers are designed for different specific applications. Among the different types of heat exchangers, the shell and tube heat exchanger would normally be used for many continuous systems having small to medium heat duties. However, in this present study a helical coil heat exchanger was selected. Because of its higher heat transfer rates as compared to a straight tube heat exchanger and following advantages [43] [47] [41].

- Enhanced heat transfer and compactness in structure
- Accommodate large heat transfer surface area in a small space
- Easy to integrate with the system, simple design and manufacturing, operation at high pressure, suitable under conditions of laminar flow or low flow rates
- Cost-effectiveness, ease of maintenance and improved thermal efficiency.

2.8.1 Geometry of Helical Coil Heat Exchanger

A helical coil can be geometrically described by pipe inner diameter 2r, coil diameter (measured between the centers of the pipes) 2R and coil pitch *P*, which is the space between consecutive coil turns (measured from the center to center) as shown in Fig 2.9 and δ is the ratio of pipe inner diameter to coil diameter [41-42].

Consider the projection of the coil on a plane passing through the axis of the coil. The angle, which projection of one turn of the coil makes with a plane perpendicular to the axis, is called the helix angle, α and φ is the angle of the tube bending in degree.

Although, consider any cross section of the pipe created by a plane passing through the coil axis. The side of pipe wall nearest to the coil axis is termed inner side of the coil and the far side is termed as the outer side of the coil pipe [41].

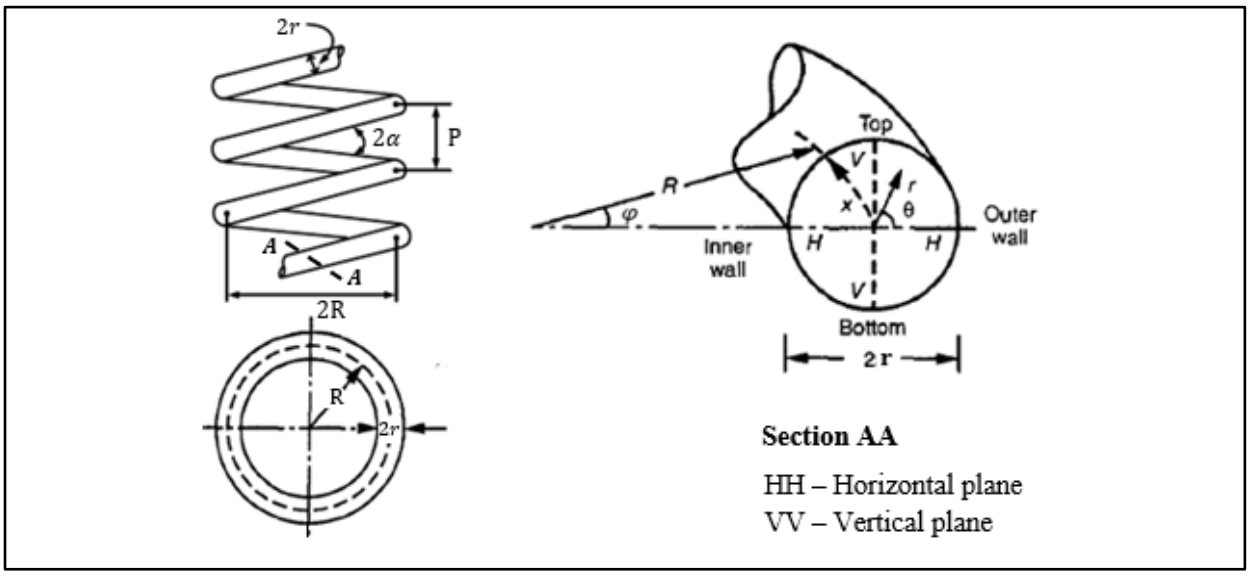

Figure 2.9: Helical coil tube with its main geometrical parameters [41]

Similar to Reynolds number of flows in pipes, Dean number is used to characterize the flow in a helical coil heat exchanger. The Dean number, De is defined as, [41].

$$De = Re\sqrt{\frac{r}{R_C}} \tag{1.1}$$

Reynolds number, Re

$$Re = \frac{2\pi u_{av}\rho}{\mu} \tag{1.2}$$

2.8.2 Heat Exchanger Pressure Drop

Kuppan, [48] explained that, the pressure drop inside the heat exchanger is the pressure loss that was not recoverable in the circuit. It also states, determination of pressure drop in a heat exchange is essential for many applications for at least two reasons.

- To identify the primary cost of the power to run fluid moving devices such as pumps, fans, and blowers which is the operating cost of a heat exchanger. This is due to the fluid pumping power, P is proportional to the exchanger pressure drop and given by [42].

  $$P = \frac{\dot{m}\Delta P}{\rho\eta_p} \tag{1.3}$$

- To study the significant heat-transfer rate influenced by the saturation temperature change for a condensing/evaporating fluid for a large pressure drop.

Where, P is the fluid pumping power, Watt, $\dot{m}$ is the mass flow rate, Kg/s, ΔP is a total pressure drop, ρ is the density of the fluid, and η_p is the efficiency of the pump.

2.9 Literature Review Summary

In this chapter, some previous researchers' studies are discovered related to Ethiopian dairy sector research gaps, solar water heating system and some background information about milk pasteurization. However, some experimental investigations are also performed to pasteurize fluid milk using solar energy in different mechanisms as follows to destroy microorganism that easily spoils milk.

Wayua, et. al [49] studied, on performance analysis of hot water jacketed solar assisted milk pasteurization in Kenya. They investigate experiment by varying the volume of milk between 20 lt to 70 lt and the maximum milk temperature obtained inversely varied from $81.4\ ^0\text{C}$ to 41.7^0C respectively. And the hot water temperature also between 40 to $73\ ^0\text{C}$ heated by flat plate solar collector with the available solar energy of an area from 700 to 1,000 W/m^2.

Atia, et.al [11] conduct experiment with flat plate solar collector and using milk itself, as a working fluid heated by collector in Egypt. They obtained for selected month of the year $63\ ^0\text{C}$ and 72^0C pasteurization temperature for 73.9 lt /day and 37.3 lt/day respectively.

In summary, this research aims to study the system described in Fig 3.3, in which a coil heat exchanger is directly immersed into the milk storage tank that used as the main heat transfer medium between the hot water inlet through coil and the raw milk in the tank to study the performance analysis of milk temperature without varying the daily quantity of milk being heated for each month of the year.

CHAPTER THREE

METHODOLOGY

3.1 Introduction

This chapter introduces the method employed and details numerical expressions of the overall modelled solar milk pasteurization system considered, to achieve the research objective mentioned in Chapter one. Fig: 3.1 show the schematic diagram of the conceptual framework of the applied methodologies, which was separated into three main parts: (1) Data collection and clustering, (2) System description and Mathematical modelling of the main components and, (3) MATLAB code developing for system performance analysis.

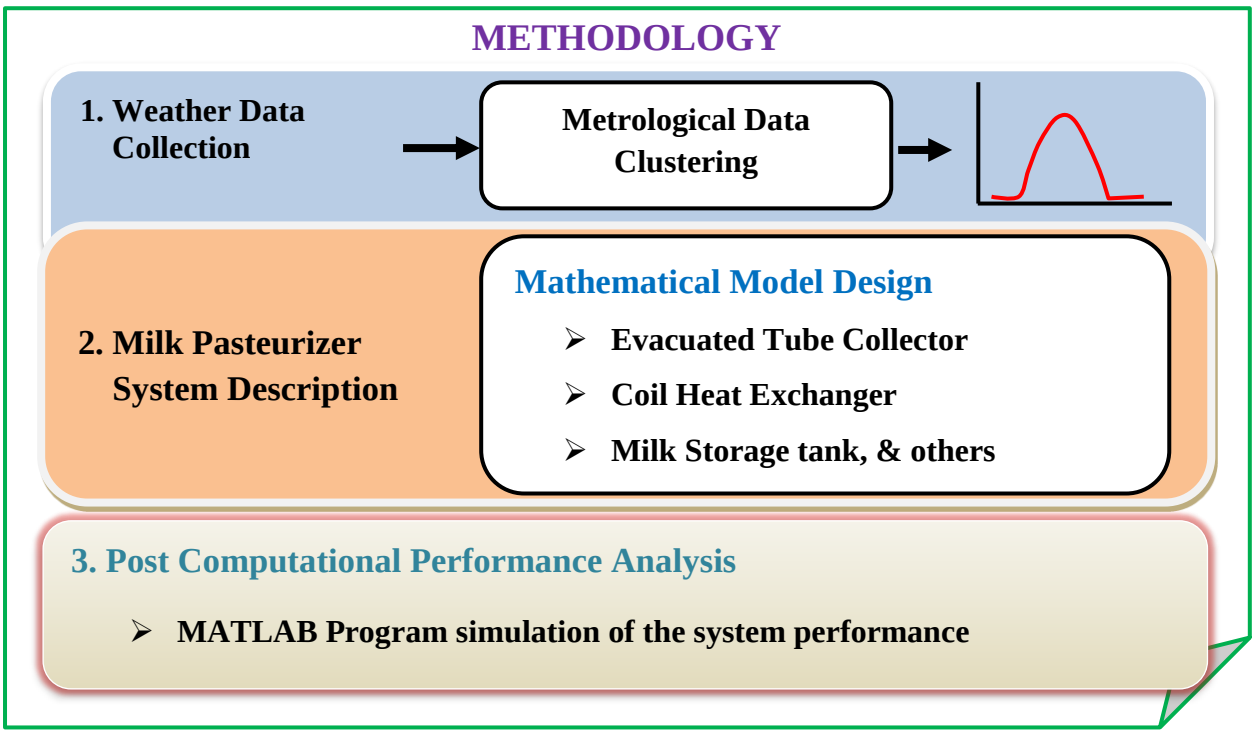

Figure 3.1: Methodology applied for the underlying study

Data collection:

This section refers to the first part of the underlying methodology, weather data gathering such as, ambient temperature, sunshine hours and geographical site location, etc. Then, clustering the meteorological data to estimate the available solar radiation in KWh/m^2 on a horizontal surface, average monthly solar radiation on inclined surface and the useful energy gained by the collector for the study location using MATLAB programming software.

System Description and Mathematical model design:

In this section, the working principle of milk pasteurizer was described. Next, mathematical model design of main components such as solar thermal collector, coil heat exchanger sizing (in chapter four) and milk storage tank analysis are performed.

Finally, **computational performance analysis** of the system was done by MATLAB coding to analysis the overall system performance (in Chapter five).

MATLAB (MATrix LABoratory) is a commercially available Simulink tool used by many researchers to generate steady state and transient response solar systems. MATLAB software also extensively used for processing of the raw data, generation of 2D plots and for solving complex mathematical equations.

Aboulmagd, et.al [35] employed MATLAB environment for a new model evacuated tube solar collector performance and obtained a good predicting accuracy of the model with experimental data measured at the same conditions.

In similar manner, Azimi, et.al [50] carried out Genetic Algorithm MATLAB software for performance optimization of single-phase evacuated tube solar collector system efficiency and for solar radiation analysis under different climatic conditions. Momale, et.al [51] develop a MATLAB code, to analysis heat transfer coefficient and correlations of a helical coil heat exchanger and also state that, numerical simulation is the most efficient and economical way for flow and thermal analysis.

Moreover, Yadav, et.al [34] developed a MATLAB simulation for Evacuated tube solar collector performance analysis via experimental data comparison to study atmospheric condition variation on useful energy gained.

For these and other reasons, MATLAB (Inc., version R2017a) computing environment was selected for analyzing the performance of the system studied, to solve complex mathematical equations and to generate final output simulation results of the overall system.

3.2 Location of the Study Area

The study was conducted for off grid per urban milk producer nearby of Kombolcha, 5 to 10 km from center of the town found in Amhara Regional State, South Wollo of Ethiopia. The area was located at 11°084′N, latitude, 39°72′ E longitude and an elevation of 1857m above sea level. The study area has warm climatic zone with dry moisture and the average monthly ambient temperature range between 25.7 ^{0}C to 33.2 ^{0}C. However, the solar energy potential in this location was high, but the precise information on global solar radiation on horizontal and inclined surfaces are not recorded previously.

3.3 Estimation of Solar Radiation

Solar radiation data is necessary for any solar conversion device design and to determine the level of solar radiation at given location and the amount of energy actually available at various orientations of the collector.

According to Duffie, et.al [52] the most common measurements of solar radiation is a total solar radiation on a horizontal surface, often referred to as global radiation on the surface. However, there are different methods to predict the amount of solar radiation reaching the Earth's surface at a given location.

Attempts have therefore been made to develop empirical relations for estimating radiation from weather data: temperature, humidity, sunshine hour, cloudiness and precipitation, which are actually easier to measure and are available at many locations.

Global Solar Radiation

One of the simplest, which also gives the smallest percentage error for the estimation of the global solar radiation from sunshine hour data, is the well-known Angstrom correlation, which can be given by Equation (3.1) [52].

$$\frac{\mathrm{H}}{\mathrm{H_O}} = a + b\frac{S}{T_d} \tag{3.1}$$

In addition, a and b are regression coefficients depend on the location and expressed as a function of latitude and sunshine hours respectively as following.

Regression Coefficients

$$a = -0.309 + 0.539cos\phi - 0.0693 * z + 0.290\frac{s}{T_d} \tag{3.2}$$

$$b = 1.449 - 0.553cos\phi - 0.694\frac{s}{T_d} \tag{3.3}$$

Where: H = global solar radiation on a horizontal surface (KWh/m^2)

Ho = extraterrestrial solar radiation on a horizontal surface (KWh/m^2)

S = sunshine hour of the day,

Z = elevation above sea level (1857m)

$\emptyset$ = latitude of the location (11.084^0)

Sunshine Duration

The maximum possible sunshine duration T_d was calculated using the following equation:

$$T_d = \frac{2}{15}\omega_s \tag{3.4}$$

Sunset Hour Angle

The sunset hour angle in degree, ω_s can be calculated by using equation (3.5) and the values for each month of the year are tabulated in Table 3.1 for the study location.

$$\omega_s = cos^{-1}(-tan\phi * tan\delta) \tag{3.5}$$

Declination Angle

The declination angle δ, is the angular position of the sun at solar noon, with respect to the plane of the equator. Its value in degrees for n, average number of the days in the month (Table 3.2) is given by the Cooper's equation:

$$\delta = 23.45 sin\left[360\frac{284+n}{365}\right] \quad (3.6)$$

Table 3.1: Sunset hour angle of the location

Sunset Hour Angle ω_s											
Jan	Feb	Mar	Apr	May	Jun	Jul	Aug	Sep	Oct	Nov	Dec
85.71	87.41	89.53	91.86	93.82	94.79	94.36	92.69	90.43	88.1	86.15	85.23

Table 3.2: Recommended average days for months and values of n by months

Month	***n* for ith Day of Month**	**For average Day of Month**		
		Date	***n***	***δ***
January	*i*	17	17	-20.9
February	31 + *i*	16	47	-13
March	59 + *i*	16	75	-2.4
April	90 + *i*	15	105	9.4
May	120 + *i*	15	135	18.8
June	151 + *i*	11	162	23.1
July	181 + *i*	17	198	21.2
August	212 + *i*	16	228	13.5
September	243 + *i*	15	258	2.2
October	273 + *i*	15	288	-9.6
November	304 + *i*	14	318	-18.9
December	334 + *i*	10	344	-23

Source [52]

Extraterrestrial Radiation

Daily extraterrestrial radiation on a horizontal surface, H_o can be computed for the day of year n is given by Equation (3.7) [52].

$$H_O = G_{sc}\frac{24}{\pi}\left[1+0.033cos\frac{360n}{365}\right]\left[\frac{\pi\omega_s}{180}sin\phi sin\delta + cos\phi cos\delta cos\omega_s\right] \quad (3.7)$$

Where G_{sc} = solar constant (1367 Wm^{-2})

Figure 3.2: shows the annual average global solar radiation on the horizontal surface in KWh/m^2 estimated with a MATLAB code developed under Appendix A having sunshine hours, declination angle and location coordinate data from Ethiopia National Metrology Agency for the period 2012 to 2016.

As seen in the figure the global solar radiation on the horizontal surface is around 0.84 KWh/m^2, which mean that, the annual average solar radiation intensity of the location reaches its maximum value 840Wh/m^2 attained at solar noon between 12hrs to 13 hrs. However, the hourly average solar radiation on inclined surface and useful energy on solar collector are is also studied and discussed under chapter five for each average month of the year.

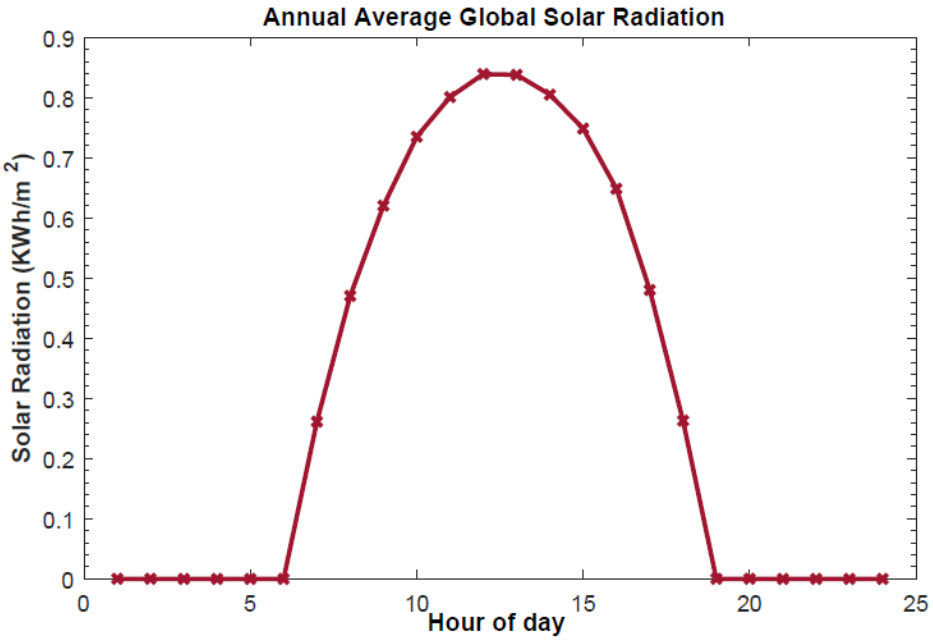

Figure 3.2: Annual Solar Radiation, Kombolcha, Ethiopia

3.3.1 Estimation of Daily Diffuse and Beam Radiation

From Table 3.1, the sunset hour angle ω_s, is greater than 81.4^0 because of that the clearness index (K_T) which is the ratio of a particular day's radiation to the extraterrestrial radiation for that day is expressed with Equation (3.8) [52].

$$K_T = \frac{\text{Daily total radiation}}{\text{Daily Extraterrestrial}} = \frac{H}{H_O} \tag{3.8}$$

Daily diffuse radiation: for sunset hour greater than 81.4^0 and $0.3 \leq K_T \leq 0.8$

$$\frac{H_d}{H} = 1.0 - 0.2832K_T - 2.5557K_T^2 + 0.8448K_T^3 \tag{3.9}$$

Daily beam radiation can be also calculated from the total daily solar radiation as follows:

$$H = H_b + H_d \tag{3.10}$$

3.3.2 Estimation of Hourly Global Radiation

For estimation of hourly solar radiation, *I* from daily data, the ratio of hourly total to daily total radiation, r_t as a function of day length and the hour is given as following.

$$r_t = \frac{I}{H} \tag{3.11}$$

Where: r_t is represented by the following equation from Collares-Pereira and Rabl (1979):

$$r_t = \frac{\pi}{24}(a + b\,cos\omega)\frac{cos\omega - cos\omega_s}{\sin\omega_s - \frac{\pi\omega_s}{180}\cos\omega_s} \tag{3.12}$$

Where: ω is the hour angle in degrees for the time under the study given by equation 15 and the coefficients *a* and *b* are expressed as:

$$a = 0.409 + 0.5016\sin(\omega_s - 60) \tag{3.13}$$

$$b = 0.6609 - 0.4767\sin(\omega_s - 60) \tag{3.14}$$

Hour Angle

The expression for the hour angle is given by the following:

$$\omega = (ST - 12) * 15 \tag{3.15}$$

Where,

H_d = Diffuse radiation

H_b = Beam radiation

ST = local solar time.

3.3.3 Estimation of Hourly Diffuse Radiation

To estimate the hourly average diffuse radiation from the ratio of hourly diffuse, I_d to daily diffuse radiation H_d, expressed by the following equation.

$$r_d = \frac{\pi}{24}\frac{\cos\omega - \cos\omega_s}{\sin\omega_s - \frac{\pi\omega_s}{180}\cos\omega_s} \tag{3.16}$$

$$r_d = \frac{I_d}{H_d} \tag{3.17}$$

3.3.4 Total Solar Radiation on Inclined Solar Collector

The total solar radiation incident on an inclined surface I_T, is a combination of the following parameters.

- Beam radiation (I_b) or direct radiation: The solar radiation propagating along the line joining receiving surface and the Sun;

- Diffuse radiation (I_d): The solar radiation scattered by dust, aerosols, and molecules, etc. and it does not have any particular direction of propagation
- Solar radiation reflected from the ground and the surrounding.

And, can be obtained from the formulae given by Liu and Jordan [52].

$$I_T = I_b R_b + I_d R_d + \rho_g R_r (I_b + I_d) \quad (3.18)$$

Where, Rb, Rd and Rr are known as conversion factors for the beam, diffuse, and reflected components, respectively; and ρ is the reflection coefficient of the ground equal to 0.6. The expressions for Rb, Rd and Rr are given below:

Beam radiation factor, R_b:

The ratio of beam radiation on the tilted surface to a horizontal surface at any time, can be calculated by Equation. (3.21). Where, beam radiation incident on a horizontal surface, I_{bh} and beam radiation incident on an inclined surface, I_{bi} are given respectively as:

$$I_{bh} = I_N(cos\theta_z) \quad (3.19)$$

$$I_{bi} = I_N(cos\theta_i) \quad (3.20)$$

Therefore, the beam radiation factor,

$$R_b = \frac{cos\theta_i}{cos\theta_z} \quad (3.21)$$

Angle of Incidence, θ_i

It is the angle between the beam radiation on a surface and normal to that surface and in simplified form given by Equation (3.22) [53].

$$\cos\theta_i = (\cos\emptyset\cos\beta + \sin\emptyset\sin\beta\cos\gamma)\cos\delta\cos\omega + \cos\delta \sin\omega \sin\beta \sin\gamma + \sin\delta(\sin\emptyset\cos\beta - \cos\emptyset\sin\beta\cos\gamma) \quad (3.22)$$

Zenith Angle, θ_z

The angle between the vertical and the line to the sun, that is, the angle of incidence of beam radiation on a horizontal surface.

$$cos\theta_Z = cos\emptyset\ cos\delta\ cos\omega + sin\emptyset\ sin\delta \quad (3.23)$$

Diffuse radiation factor, R_d: is the ratio of diffuse radiation on the tilted surface to that on the horizontal surface.

$$R_d = \frac{1 + cos\beta}{2} \quad (3.24)$$

Reflected radiation $\mathbf{R_r}$, from the ground and other surrounding objects on the solar surface is expressed as:

$$R_r = \frac{1 - cos\beta}{2} \tag{3.25}$$

Where, β is the tilt angle between the plane of the surface in question and the horizontal.

Tilted Angle

The optimal tilt angle obtained by Duffie and Beckman as function of the latitude ($\emptyset$) was used by many researchers for different locations is given by [54].

$$\beta_{opt} = (\emptyset + 15^0) \tag{3.26}$$

Suppose as seen Fig 3.2, the solar time of the location is more over at 1:30PM or 13:30hr, Therefore, using Equation (3.15) hour angle of the study location and the tilted angle are calculated as follows:

$$\omega = (ST - 12) * 15 = 22.5^0$$

Then, tilt angle: $\beta = (11.084^0 + 15) \approx 26.1^0$

Substituting Equations from (3.19) to (3.26) into Equation(3.18) and rewriting total solar radiation on inclined surface also estimated by using equation (3.27) in terms of the global radiation (H), diffuse radiation (H_d), beam radiation factor (R_b) and ground reflectivity factor (ρ) as follows: [53].

$$I_T = R_b(H - H_d) + 0.5(1 + cos\beta)H_d + 0.5\rho(1 - cos\beta)H \tag{3.27}$$

3.4 Estimation of Hourly Ambient Temperature

The performance of a solar thermal collector depends considerably on the temperature of external air and knowing just the average monthly value is not enough. Therefore, the method was developed to calculate the hourly ambient temperature from the daily ambient temperature given by Parton and Logan [55]. Since, it is assumed that the temperature trend of the day was both heating during daylight hours and cooling during night time. Therefore, the two hourly variables are expressed as follows:

For day light hours:

$$T(h) = T_{min} + (T_{max} - T_{min})sin\left(\frac{\pi m}{y + 2a}\right) \tag{3.28}$$

For night time hour:

$$T(h) = T_{min} + (T_{Sunset} - T_{min})Exp\left(-\frac{bn}{z}\right) \tag{3.29}$$

Where: T(h) is the temperature at any hour of the day or night period determined from m and n. y and z are day (h) and night length (h) respectively, T_{Sunset} is temperature at sunset (^0C), m is the number of hours between time at T_{min} and sunset (h), n is the number of hours from sunset to the time of T_{min}(h) and a, equal to 1.80h is lag coefficient for T_{max}, b, equal to 2.20 h is night – time temperature coefficient c, equal to 0.880h is the lag time of T_{max} from time of sunrise

3.5 Model System Description

Fig: 3.3 shows a schematic diagram of solar milk pasteurizer system considered. In this system, an evacuated tube solar collector with thermal storage tank, milk storage tank, an immersed coil heat exchanger and circulating pump are the main components including the pipe lines.

In the diagram shown, an evacuated tube solar collector was inclined at 26.1^0transfer thermal energy captured by glass tubes using water as heat transfer fluid. In this process thermosiphon circulation was performed after the working fluid enters the U-tubes inlets and evenly distributed, it absorbs heat and the water temperature rise in glass outlet tubes then inlet to the manifold [35].

Then, the hot water stored in the manifold or thermal storage tank was utilized by coil heat exchanger for raw milk heating, which is the main heat transfer medium and placed at the bottom of the milk storage tank.

Afterward, the return hot water from coil out let was pumped to the thermal storage tank to be reheated up again by glass tubes. The cylindrical milk storage tank has a 100-liter milk holding capacity and well insulated so as to avoid heat loss to the surrounding. It also, an openable lid at the top and a pipe line at the bottom for the pasteurized milk outlet as shown below.

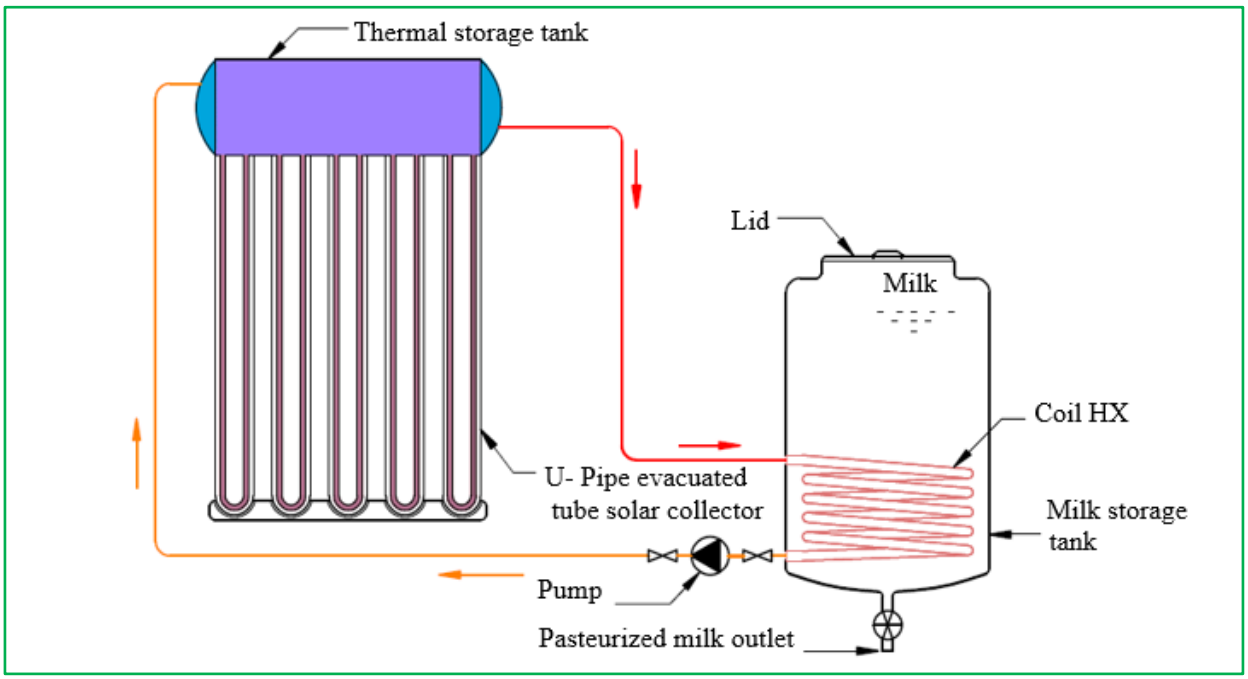

Figure 3.3: A schematic of milk pasteurizer system studied

In general, the batch type milk pasteurizer system explained above and displayed in Fig: 3.3 was mainly composed of three units such as an Evacuated tube solar collector, coil HX and milk storage tank. Moreover, mathematical model design, thermal analysis and some component sizing were discussed in the next sub sections to study the overall system performance based on the solar energy of the location and the milk volume specified with MATLAB software.

3.6 Mathematical Model Design of an Evacuated Tube Solar Collector

As mentioned in Chapter 2, all solar thermal systems possess some form of solar collector to convert incident solar radiation into thermal energy to increase the temperature of the working fluid. As explained by many researchers, evacuated tube solar collector offers a much higher thermal efficiency in different condition as compared to flat plate collector to fulfill the hot water requirement for heating process. For these reasons, an evacuated tube collector was selected for this research study.

The following several assumptions are made to simplify mathematical simulation.

- The flow rate distributes evenly among the tubes of the collector
- All the tubes exhibit the same thermal performance.
- Absorption of the glass is negligible and heat conduction loss of the retaining clip is negligible.
- The heat transfer between the two legs of the inlet and outlet sides is negligible.
- The thermos physical properties are constant and the thermal mass is negligible owing to the thin walls of the glass tube, the aluminum fins and the copper tube.
- The heat transfer rate through the tubes is assumed to be isothermal
- Ambient air temperature is from metrology agency

3.6.1 Governing Equations of the Solar Collector

For predicting the behavior of solar collector at any time step, thermal network is formed for calculating the heat transfer in any direction of the tube from the solar collector differential equation [56]. Figure 3.5, shows a schematic of heat transfer mechanism in an evacuated tube solar collector from the absorber tube to glass envelope and from envelope to surroundings and in that of fluid temperature is considered as a function of x. Figure 3.6, gives the mode of the thermal network associated with the heat transfer process of the collector.

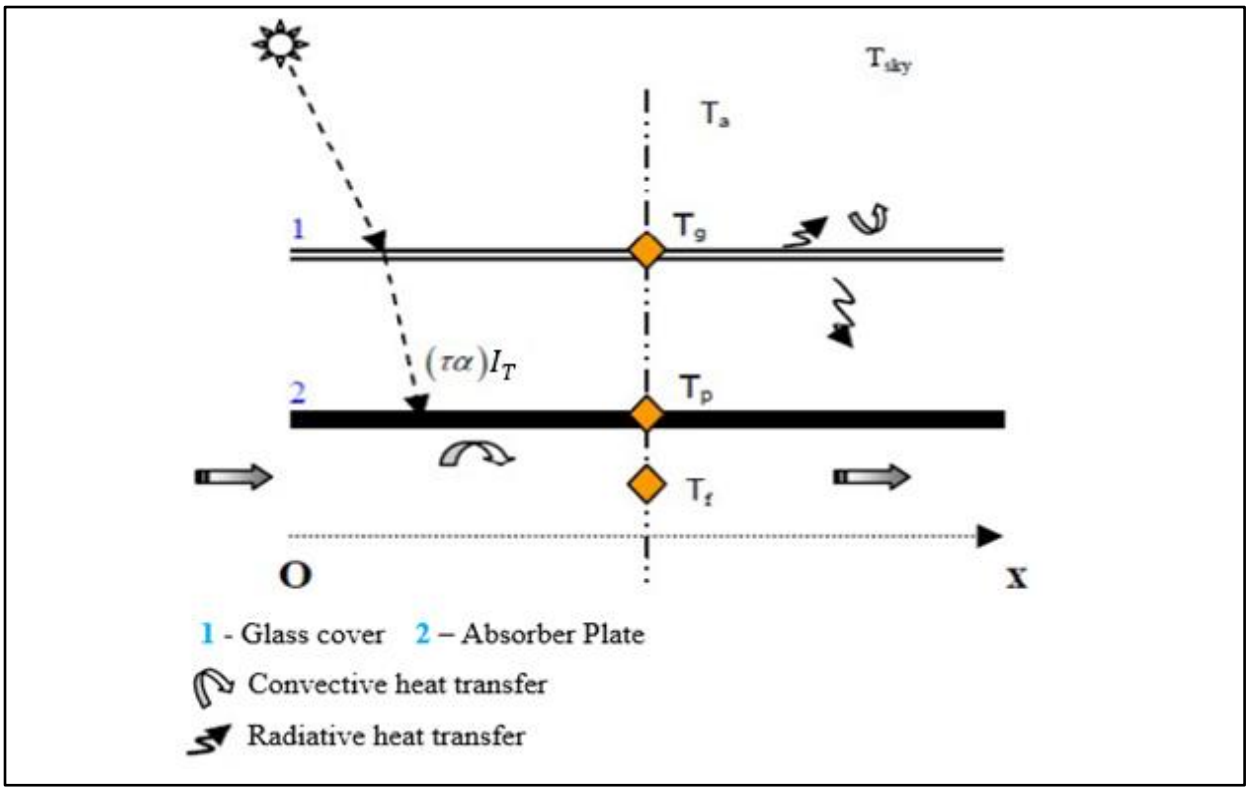

Figure 3.4: Heat transfer mechanism in evacuated tube solar collector [56]

The governing differential equations for determining the glass temperature,T_g, the absorber plate, T_p and the fluid temperature, T_f at any time t step are as follows: [56]

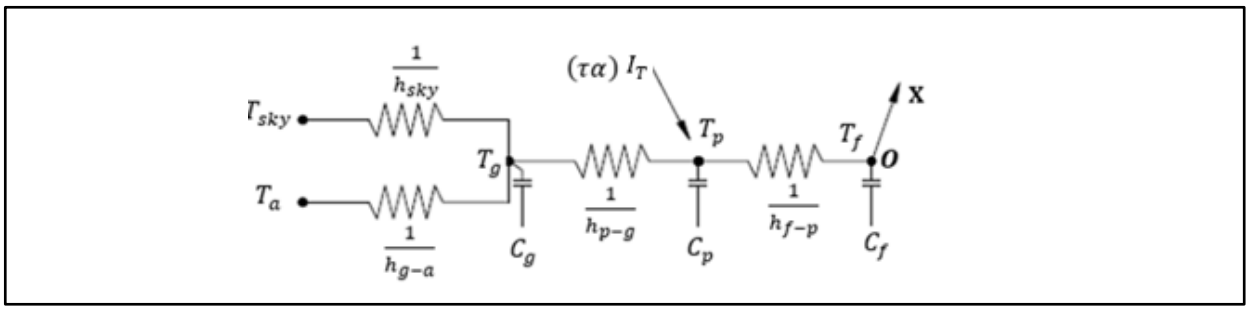

Figure 3.5: Thermal Networks for the 3-Node Model

Glass Temperature Equation

$$C_g \frac{\partial T_g}{\partial t} = \varepsilon_g \sigma\left(T_{sky}^4 - T_g^4\right) + h_{g-a}\left(T_a - T_g\right) + \varepsilon_g \sigma\left(T_p^4 - T_g^4\right) \tag{3.30}$$

Plate Temperature Equation

$$C_p \frac{\partial T_p}{\partial t} = \tau\alpha\, I_T + \varepsilon_g \sigma\left(T_g^4 - T_p^4\right) + h_{f-p}\left(T_f - T_p\right) \tag{3.31}$$

Fluid Temperature Equation

$$C_f \left(\frac{\partial T_f}{\partial t} + u \frac{\partial T_f}{\partial x}\right) = h_{f-p}\left(T_p - T_f\right) \tag{3.32}$$

The temperature of the water, leaving the solar collector at any time ***t*** is determined using Equation (3.33) through making an energy balance of the water stream, as following:

$$\left(\dot{m}C_p\right)_w = \frac{dT_f}{d_t} = A_c * h_{f-p}\left(F_w * T_p - \frac{T_f + T_{fi}}{2}\right) - \left(\dot{m}C_p\right)_w\left(T_f - T_{fi}\right) \quad (3.33)$$

Here,

$F_w = 2\eta_f - 1$, Where η_f is the fin efficiencies, C_g is heat capacity of glass cover (KJ/m²·K), C_p is heat capacity of absorber (KJ/m²·K), I_T is global solar irradiance in the plane of the collector (KW/m²), h_{f-p} is heat transfer coefficient fluid – absorber (KW/m²·K), h_{g-a} is heat transfer coefficient glass – ambient (KW/m²·K), T_a is the ambient temperature (°C), T_{sky} is the sky temperature (°C), α is absorptive coefficient, ε is emissivity, σ is the Stefan-Boltzmann constant ($5.67 \times 10^{-8} W.m^{-2}K^{-4}$).

3.6.2 Hourly Thermal Energy Output

The absorbed solar radiation per unit area $\left(\dot{Q}_{Abs}\right)$ is the sum of the useful heat gained $(\dot{Q}_u)$ by the working fluid and the thermal loss per unit area of the absorber $\left(\dot{Q}_{loss}\right)$ is given as follows: [35].

$$\dot{Q}_{Abs} = \dot{Q}_u + \dot{Q}_{loss} \quad (3.34)$$

3.6.3 Useful Solar Energy

The amount of energy required to raise the working fluid temperature or utilized energy is equal to the amount of energy that solar collector could absorb. The rate of utilized energy by solar collector transferred to the fluid is expressed as follows: [57]

$$\dot{Q}_u = \dot{m} * C_p * (T_{out} - T_{in}) \quad (3.35)$$

Using the collector heat removal factor (F_R) and the overall heat loss coefficient (U_L) the useful rate of energy ($\dot{Q}_u$) also expressed by Equation (3.36)

$$\dot{Q}_u = A_{ab}F_R\left[I_T(\tau\alpha) - U_L\left(T_{ig} - T_a\right)\right] \quad (3.36)$$

Absorber area, A_{ab} is expressed as:

$$A_{ab} = d_g x L \quad (3.37)$$

Absorbed Solar Energy

The total solar energy received by absorber plate in evacuated tube solar collector is given by Equation (3.38) [56] [58].

$$\dot{Q}_{abs} = (\alpha\tau)I_T A_{abs} \quad (3.38)$$

Where, $\dot{m}$ is the mass flow rate of water, C_p is the heat capacity of water, T_{in} and T_{out} refers to the inlet and outlet water temperature, respectively, and $\tau\alpha$ is the transmittance - absorptance product and ε is the emissivity of the selective surface layer. The value used for the product $\tau\alpha$ is 0.837 [58].

3.6.4 Overall Heat Loss Coefficient

In Eq. (3.36) the overall heat loss coefficient (U_L) is defined as the sum of top loss coefficient and edge loss coefficient given as follows: [35].

$$U_L = U_{top} + U_{edge} \tag{3.39}$$

However, the edge loss coefficient was neglected due to the assumption of proper heat insulation at the edges of the solar collector. Therefore, the top loss coefficient from the absorber tube to the ambient, U_{top} can be written as:

$$U_L = U_{top} = \left(\frac{1}{h_{g-a,conv}} + \frac{1}{h_{p-g,rad}} + \frac{1}{h_{g,cond}}\right)^{-1} \tag{3.40}$$

Where $h_{g-a,conv}$ is the heat transfer coefficient between the outer glass tube and the ambient due to convection (W/m^2 K), $h_{p-g,rad}$ is radiation heat transfer coefficient between the absorber tube and the outer glass tube (W/m^2 K) and $h_{g,cond}$ is the conduction heat transfer coefficient between the inner glass tube and the fin.

- Radiation heat transfer coefficient from the absorber plate to the outer glass tubes can be given by Equation (3.42) [35].

$$h_{p-g,rad} = \frac{\sigma\varepsilon_{ig}}{1 + \frac{\varepsilon_{ig}d_p}{\varepsilon_{og}d_g}\left(1-\varepsilon_{og}\right)}\left(T_{ig}^2 + T_{og}^2\right)\left(T_{ig} + T_{og}\right) \tag{3.41}$$

  This also expresses as:

$$h_{p-g,rad} = \varepsilon_{ig} - \varepsilon_{og}\sigma\frac{\left(T_{ig}^4 - T_{og}^4\right)}{\left(T_{ig} - T_{og}\right)} \tag{3.42}$$

  The term,

$$\varepsilon_{ig} - \varepsilon_{og} = \left\{\frac{1}{\varepsilon_{ig}} + \frac{\varepsilon_{ig}}{\varepsilon_{ig}}\right\} \tag{3.43}$$

- Radiation heat transfer coefficient from glass to ambient air [34]

$$h_{g-a,rad} = \varepsilon_{ig}\sigma\left(T_g^2 + T_a^2\right)\left(T_g + T_a\right) \tag{3.44}$$

- Absorber tube temperature, T_{ig} and has been taken as the average of inlet and outlet fluid temperature

$$T_{ig} = T_m = \frac{T_{fi} + T_{fo}}{2} \tag{3.45}$$

- Radiation heat transfer coefficient to the sky, $h_{g-a,rad}$ can be given as:

$$h_{g-a,rad} = \sigma\varepsilon_g\left(T_g^2 + T_{sky}^2\right)\left(T_{og} + T_{sky}\right) \tag{3.46}$$

- The sky temperature, T_{sky} is given as follows:

$$T_{sky} = T_a - 6 \tag{3.47}$$

- The glass temperature, T_g can be formulates as:

$$T_g = T_{ig} - U_L\left(\frac{T_{ig} - T_a}{h_{g-a,rad}}\right) \tag{3.48}$$

- Forced convection heat transfer coefficient on outer tube by the wind, h_{g-a},

$For\ 0 \le V_w \le 5m/s$

$$h_{g-a} = 5.7 + 3.8V_w \tag{3.49}$$

Where,

ε_{ig} = the emissivity of the selective absorbing coating,

ε_{og} = the emissivity of the inner surface of outer glass tube

V_w = ambient air velocity in m/s.

Thermal Energy Lost from Absorber Tube

In general, the rate of thermal energy lost from the absorber tube using the overall heat loss coefficient is given by Equation (3.50) [56].

$$\dot{Q}_{thermal-loss} = U_L A_{ig}\left(T_{ig} - T_a\right) \tag{3.50}$$

Where A_{ig} = the area of the inner glass tube,

T_{ig} = temperature of the inner glass tube

Thermal Energy Loss from Manifold Header

The energy loss from the thermal storage tank or manifold header to the ambient for the hot fluid temperature inlet to the manifold header can be calculated using Equation (3.51) [58].

$$\dot{Q}_{loss,manifold} = U_S A_S\left(\mathrm{T_{wo}} - \mathrm{T_a}\right) \tag{3.51}$$

Where, $U_S A_S$ = storage tank's overall heat transfer coefficient-area product

$T_{wo} - T_a$ = temperature difference between the tube outlet and ambient temperature

The overall heat transfer coefficient, U_S of Equation (3.52) is expressed as:

$$U_S = \frac{1}{\frac{1}{h_{ci}} + \frac{e_1}{K_1} + \frac{e_2}{K_2} + \frac{e_3}{K_3} + \frac{1}{h_{co} + h_r}} \tag{3.52}$$

$$h = 5.7 + 3.8V_w \tag{3.53}$$

$$h_r = \varepsilon\sigma(T_s^4 - T_a^4) \tag{3.54}$$

Where:

h_{ci} = Convective heat transfer coefficient inside the header

h_{co} = Convective heat transfer coefficient due to the wind outside the header cover

h_r = Heat transfer coefficient due to radiation losses

ε = Emissivity of the cover

T_s = Temperature of the external surface

e_1, e_2 *and* e_3 are the thicknesses of the various layers of material including the construction of the header, the insulation material and the external cover respectively.

K_1, K_2 and K_2 are the thermal conductivities of those materials respectively.

However, the various layer of manifold construction materials physical properties are listed in Table C.2.

3.6.5 Collector Efficiency

By using the useful heat gain, solar radiation on inclined surface and solar collector area, A_c the thermal efficiency (η) of the solar collector can be calculated by using Equation (3.55) [57].

$$\eta = \frac{\dot{Q}_u}{A_c * I_T} = \frac{\dot{m} * C_p * (T_{out} - T_{in})}{A_c I_T} \tag{3.55}$$

Using the useful rate of energy ($\dot{Q}_u$) of Equation (3.36)

$$\eta = F_R(\tau\alpha) - F_R U_L \left(\frac{T_{in} - T_a}{I_T}\right) \tag{3.56}$$

However, in reality the heat loss is not constant, but linearly depends on the difference between the inlet and ambient temperatures and the product $F_R U_L$ were calculated as:

$$F_R U_L = a_1 + a_2(T_{in} - T_a) \tag{3.57}$$

Substituting Equation (3.57) into (3.56), the general form of the thermal collector efficiency can be re-arranged as follows:

$$\eta = \eta_0 - a_1 \frac{(T_{in} - T_a)}{I_T} - a_2 \frac{(T_{in} - T_a)^2}{I_T} \tag{3.58}$$

The term η_0 is collector optical efficiency, a_1 and a_2 are thermal loss parameters. Technical specifications of the solar thermal collectors are listed in Table: 3.3.

Table 3.3: Technical Specifications of the Solar Thermal Collector

Parameter	Value	Unit
η_0	0.63	[-]
a_1	1.24	$[W/m^2k]$
a_2	0.009	$[W/m^2k^2]$

3.6.6 Solar Thermal Collector Heat Balance Equations

The thermal model of heat balance equations for each part of evacuated tube solar collector, based on Ref. [31-32] expressed below as follows:

(1) Outer Glass Tube

$$h_{i-o}P_{i-o}(T_i - T_o) + h_{o-a}P_o(T_a - T_o) = 0 \quad (3.59)$$

Here,

$$h_{i-o} = h_{i-o,rad} + h_{i-o,cond} \quad (3.60)$$

$$h_{o-a} = h_{o-a,rad} + h_{o-a,conv} \quad (3.61)$$

$$P_{i-o} = \frac{(P_i + P_o)}{2} \quad (3.62)$$

Where, $T_i, T_{o,}\ and\ T_a$ are the inner glass tube temperature, outer glass tube temperature and ambient temperature respectively; h_{i-o} is the heat transfer coefficient between the inner and outer glass tube and h_{o-a} is the heat transfer coefficient between the outer glass tube and the ambient environment. However, heat conduction can be ignored because of a very narrow vacuum layer space between the inner and outer tubes, in which the vacuum level is 10^{-4}Pa and the heat conduction coefficient is less than $0.27 * 10^{-5} W/m\ ^0C$.

The term $h_{i-o,rad}$ and $h_{i-o,cond}$ are the radiation and conduction heat transfer coefficients between the outer and inner glass tube, and $h_{i-o,cond}$ is treated as zero, $h_{o-a,rad}$ and $h_{o-a,conv}$ are the radiation and convection heat transfer coefficients between the outer tube and the ambient environment, $h_{o-a,conv}$ is a function of the wind velocity, $P_i\ and\ P_o$ are the

perimeters of the inner and outer glass tubes

(1) Inner Glass Tube

$$h_{i-o}P_{i-o}(T_o - T_i) + h_{i-Al}P_{i-Al}(T_{Al} - T_i) + Q_{edge} + \tau_g\alpha_i d_g s = 0 \quad (3.63)$$

Here,

$$h_{i-Al} = h_{i-Al,rad} + h_{i-Al,cond} \quad (3.64)$$

$$P_{i-Al} = \frac{(P_i + P_{Al})}{2} \tag{3.65}$$

$$Q_{edge} = h_{i-a} P_i (T_a - T_i) \tag{3.66}$$

Where T_{Al} is the aluminum fin temperature, h_{i-Al} is the total heat transfer coefficient between inner glass tube and aluminum fin, $h_{i-Al,rad}$ and $h_{i-Al,cond}$ are the radiation and conduction heat transfer coefficients between inner glass tube and aluminum fin. τ_g is the transmission coefficient of the outer glass tube; α_i is the absorption coefficient of the selective coating on the inner glass tube; d_g is the diameter of the outer glass tube; S is the total solar irradiance on the collector aperture surface; P_{Al} is the perimeter of aluminum fin, Q_{edge} is the heat loss of the tube edge to the manifold and h_{i-a} is the tube edge heat loss coefficient of the collector approximately equal to $0.6 W/m^2K$

(3) Aluminum Fin

$$h_{i-Al} P_{i-Al} (T_i - T_{Al}) + h_{Al-Cu} P_{Cu} (T_{Cu} + T_{Al}) = 0 \tag{3.67}$$

$$h_{Al-Cu} = h_{Al-Cu,rad} + h_{Al-Cu,cond} \tag{3.68}$$

The conduction heat transfer coefficient is given as:

$$h_{i-Al,cond} = \frac{k_{air}}{t_{air}} \tag{3.69}$$

Where, k_{air} and $\mathrm{t_{air}}$ are the thermal conductivity coefficient and the thickness of the air layer. $h_{i-Al,cond}$ and T_{Cu} is the U copper pipe temperature, P_{Cu} is the perimeter of the copper pipe, and h_{Al-Cu} is the total heat transfer coefficient between the aluminum fin and U copper pipe. $h_{Al-Cu,rad}$ and $h_{Al-Cu,cond}$ are the radiation and conduction heat transfer coefficients between the aluminum fin and U copper pipe respectively.

(4) U-Pipe Copper

$$h_{Al-Cu} P_{Cu} (T_{Al} - T_{Cu}) + h_f P_{Cu} (T_f - T_{Cu}) = 0 \tag{3.70}$$

Where, h_f was the fluid convective heat transfer coefficient inside the U copper pipe and this coefficient is variable with flow velocity.

(5) Working Fluid

$$h_f P_{Cu} (T_{Cu} - T_f) * X + \dot{m} C_p (T_{iwf} - T_{Owf}) = 0 \tag{3.71}$$

Where, T_{iwf} and T_{Owf} are the inlet and outlet temperatures of working fluid in the U copper pipe and X is the interval of the fluid along the tube axis. $\dot{m}$ and $C_p$are the mass flow rate and specific heat capacity of the working fluid. In addition, for each heat transfer coefficient values are given in Table C-1.

3.6.7 Technical Specification of Evacuated Tube Solar Collector

Table: 3.4 shows the properties of evacuated tube solar collector made of borosilicate glass and selective material (Al-N/Al) coated over inner tube of outer surface area for excellent solar radiation absorption, and an evacuated tube solar collector with specifications in Table 3.5 are selected for this study to analysis the performance of milk pasteurization [34] [59].

Table 3.4: Properties of Borosilicate Glass Tube

Parameters	Symbol	Values
Thermal Conductivity	K	1.125 W/mK
Solar Transmittance	τ_g	0.90
Solar Absorptance	α_g	0.92
Thermal Emittance	ε_g	0.85

Table 3.5: Structural parameters of Evacuated Tube Collector taken for simulation

S.No.	Components	Value	Unit
1	Gross area of solar collector	2.11	m^2
2	Total area of absorber tube	1.64	m^2
3	Length of tube	1500	mm
4	Number of tubes	10	--
5	Tube outer diameter	47	mm
6	Tube inner diameter	37	mm
7	Tube spacing	11.2	mm
8	Thickness of tube	2	mm

3.6.8 Thermal modelling of thermal storage tank

Storage tank plays a major role in the system performance. Assuming a fully stratified storage tank scenario, the energy balance equation is expressed as following [57].

$$\rho V_s C_p \frac{dT_s}{dt} = \dot{Q}_U - \dot{Q}_{Load} - \dot{Q}_{loss,\ thermal\ storage} \quad (3.72)$$

The thermal energy exchanged with thermal collector field is calculated with Equation (3.73) [53].

$$\dot{Q}_U = \left(\dot{m}C_p\right)_w (T_{wo} - T_{wi}) \quad (3.73)$$

Where, $V_s =$ volume of water in thermal storage tank, m^3

$T_s =$ instantaneous tank temperature

$C_p =$ is heat capacity of water, J/ (kg K)

$\dot{Q}_{LOAD}$ = load energy

CHAPTER FOUR

HELICAL COIL HEAT EXCHANGER DESIGN

4.1 Introduction

In this section, based on some numerical assumption and using the equation of logarithmic mean temperature difference method, the coil dimensional parameters are determined. Next, for studying the transient analysis with a MATLAB software basic heat transfer governing equation are also developed to generate pasteurized milk temperature.

4.2 Sizing of a Coil Heat Exchanger

Figure: 4.1 shows a schematic drawing of the milk storage tank, which consists an immersed coil heat exchanger placed at the bottom of the tank and fitted on the lateral wall of the tank. The cross sectional cut way view of helical coil heat exchange dimensional parameters are also shown in Fig: 4.2.

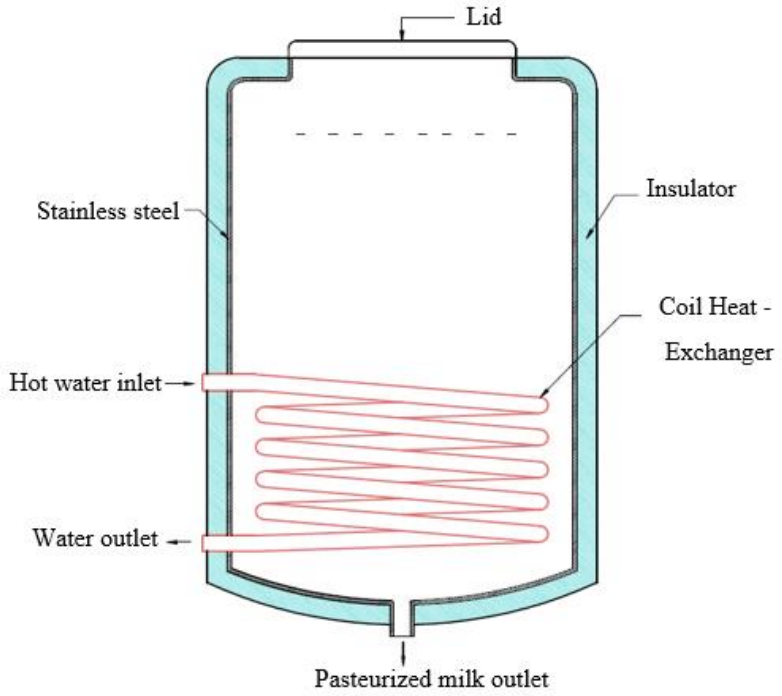

Figure 4.1: Cross sectional view of milk Storage tank

4.2.1 Coil Heat Transfer Area

For designing this kind of heat exchanger, input parameters are very important to size the helical coil heat exchanger. In this case, the first step is to calculate the coil heat transfer area, A_o from Equation (4.2). To use this equation, let assume the maximum inlet and outlet or return water temperature of the water from coil tube to be 100^0c and 73^0c respectively; and the initial milk inlet and the final temperature of milk in the storage are to be 32^0c and 68 ^{0}c respectively as used by Verechshagin, et.al [60].

The thermal output of the collector (hot water exits from the collector), transferred through coil exchanger can be calculated and expressed based on equation (4.1) [61].

$$Q = \eta * (A_c q_{sun}) \quad (4.1)$$

Where, η = efficiency of collector, for 50%

A_c = collector gross area, 2.11m^2 (Table: 3.5)

q_{sun} = the quantity of heat obtained by the collector for every square meter, and its nominal value is equal to 800W/m^2.

Using Equation (4.1), we get:

$$Q = 0.5 * 2.11 * 800$$
$$= 844 \text{ W}$$

The amount of heat transferred through the coil HX to heat the raw milk, Q was also obtained by using Equation (4.2) in terms of mean temperature difference as following.

$$Q = A_o \varepsilon U_0 \frac{\Delta T_m}{C_r} \quad (4.2)$$

$$\Delta T_m = T_{avg,cw} - T_{avg,m} \quad (4.3)$$

Where,

ΔT_m = the difference between the average temperature of circulating water inside the coil, $T_{avg,cw}$ and the average temperature of milk in the tank, $T_{avg,m}$.

ε = the coefficient of furring, which result as an uneven distribution of thermal media affect the efficiency of the heat transfer coefficient, 0.6 to 0.8 normally used 0.7.

C_r = the heat loss coefficient, 1.1 to 1.2

$$T_{avg,cw} = \frac{T_{s,f} + T_{w,r}}{2} \quad (4.4)$$
$$= (100 + 73)/2 = 86.5^0 C$$

$$T_{avg,m} = \frac{T_{mf} + T_{mi}}{2} \quad (4.5)$$
$$= (68 + 32)/2$$
$$= 50^0 C$$

Then, $\Delta T_m = 86.5 - 50 = 36.5^0 C$

The overall heat transfer coefficient for such kinds of heat exchanges was between 200 to 500 W/m^2 ^{0}C [62]. Suppose the overall heat transfer coefficient of this heat exchanger to be 450 W/m^2 ^{0}C, nominal value) then the required heat transfer area of the coil heat exchanger from Equation (4.2) can be calculated as follows.

Using the value of $C_r = 1.1$,

$$A_o = \frac{C_r Q}{\varepsilon U_0 \Delta T_m} = \frac{1.1 * 844}{0.7 * 450 * 36.5} = 0.081 m^2$$

Diameter of Copper Pipe

Using small diameter pipes instead of one large diameter pipe will provide high heat transfer area. For this heat exchanger 8mm nominal outer diameter and 0.61mm thick commercially available copper tube was selected.

Thus, $d_o = 8$ mm and

$d_i = 6.78$ mm

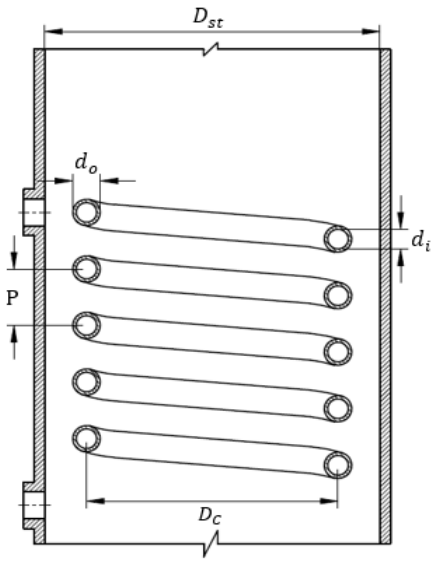

Figure 4.2: Schematic cut-away view of a helical coil heat exchanger

Coil Pitch

The pitch of the helical coil, *P* given by Equation (4.6) is a common design value in such types of heat exchangers [47].

$$p = 1.25 * d_o \tag{4.6}$$

Substituting the value of d_o,

$$p = 1.25\ x\ 8\ mm$$
$$= 10\ mm$$

Required Length of Copper Tube

The minimum required copper coil length, L_{coil} can be calculated using the outer diameter as following:

$$L_{coil} = \frac{A_o}{\pi d_o} \tag{4.7}$$

Substituting,

$$L_{coil} = \frac{0.081\ m^2}{\pi \times 0.008m} = 3.22\ m$$

Approximately the length of coil needed to make number of turns was 3.5 m.

Coil Diameter

For enhancing heat transfer efficiency with increasing number of coils turns, supposed that the coil diameter of 250 mm taken:

Number of coils turns

The number of coils turns of the heat exchanger, N_{coil} considering the coil length and the pitch as given by [47] obtained using Equation (4.8).

$$N_{coil} = \frac{L_{coil}}{\sqrt{(\pi D_c)^2 + p^2}} \tag{4.8}$$

Substituting the values in Equation (4.8),

$$N_{coil} = \frac{3.5\ m}{\sqrt{(\pi * 0.25)^2 + (0.01)^2}}$$

$$= 4.456$$

However, the actual number of coils turns needed, N_{coil} is simply rounded to the next highest integer equal to 5 turns.

The volume occupied by the coil, V_c:

$$V_c = \frac{\pi}{4} d_o^2 L_{coil} \tag{4.9}$$

$$V_c = \frac{\pi}{4}(0.008\ m)^2 * 3.5\ m$$
$$= 1.76 * 10^{-4}\ m^3$$

Volume of the Milk Storage Tank, V_{st}:

Considering the volume occupied by coil tube and the required 0.1 m^3 volume of milk in the tank can be calculated as:

$$V_{st} = V_c + 0.1 m^3 \tag{4.10}$$
$$= 0.1002\ m^3$$

Height and Diameter of Milk Storage Tank

To process 0.1 m^3 volume of milk in the vertical cylindrical tank of Fig: 4.1. let set the space difference between D_{st} and D_c to be x = 85 mm. The milk storage tank internal diameter and height are determined as follows:

Storage Internal Diameter

$$D_{st} = 2x + D_c \tag{4.11}$$
$$= \big((2 * 85) + 250\big)$$
$$= 420\ mm$$

Storage Height

Considering additional 10% of the total volume and using general Equation of (4.12) to calculate cylindrical tank volume and substituting the value D_{st} from equation (4.11) into equation (4.12), the milk storage tank height (H_{st}) can be obtained as follows:

$$V_{st} = \frac{\pi D_{st}^2}{4} * H_{st} \quad (4.12)$$

$$H_{st} = \frac{4V_{st}}{\pi D_{st}^2} = \frac{4(0.01 + 0.1002)}{\pi(0.42\ m)^2}$$

$$= 0.795$$

$$\approx 0.80\ m$$

From the above parameters the total internal volume of milk storage tank becomes;

$$V_{st} = \frac{\pi(0.42)^2}{4} * 0.80$$

$$= 0.1102\ m^3$$

$$\approx 110.2\ Lt.$$

4.3 Material selection of milk storage tank and its insulation

Dairy and food industries are concerned with reliability of equipment and product purity. This requires the use of cleanable, corrosion-resistant stainless-steel equipment to meet the needs of milk product consumers everywhere. Due to following reasons, stainless steel material was suggested for milk storage tank construction. The major characteristics of stainless steel being widely used in food and dairy industries are [63]:

- Durability and corrosion resistance
- Ease of fabrication
- Heat resistance
- Flavor and color protection; and cleanability
- Strength and ductility at ambient and service temperatures
- Total cost, including initial cost, installed cost, and the effective life expectancy of the finished product, etc.

Heat losses from the milk storage tank is also an irreversible process. Thus, thermal insulation is required to prevent heat losses from milk storage tank. However, thermal insulator is a poor conductor of heat having low thermal conductivity but, it does not eliminate heat transfer, it merely reduces it.

So, the optimum thickness of insulation to be installed was recommended based on minimum total cost as shown in Fig D.2 [64]. In Table: C.3, various thermal insulation material properties are listed; However, glass fiber insulation material is selected for the following reasons:

- Lower thermal conductivity properties
- Lower cost per unit area
- Higher temperature resistance
- Higher durability in the presence of moisture.
- Higher resistance to the water
- Cost effective and steady in performance

4.4 Coil Heat-Transfer Analysis

Previously, in order to size coil HX parameters the hot water temperature flow through the coil was assumed to be uniform, but it changing during the process at any instance of time. Moreover, the milk pasteurizer tank is carefully insulated to minimize heat losses and such losses are also assumed as negligible. However, in this sub section helical coil HX heat transfer govering equations are explored for MATLAB simulation of the system. Because, the solar energy and the ambient temperature are time dependent which result different hot water temperature exit from an Evacuated tube solar collector and entering to the coil heat exchanger for each months of the year.

4.4.1 Formulation of Heat Gain through Coil Tube

The rate of total quantity of heat exchanged throughout the entire length of the coil, $\dot{Q}$ expressed in terms of logarithmic mean temperature difference (ΔT_{LMTD}) given by equation (4.13) [42] [47].

$$\dot{Q} = U * A_o * \Delta T_{LMTD} \tag{4.13}$$

4.4.2 Calculation of Overall Heat Transfer Coefficient

The overall heat transfer coefficient, U can be described in terms of three thermal resistances referred to the outer coil surface and expressed as following [65] [66].

$$UA_O = \frac{1}{R_t} = \left(\frac{1}{\pi d_o L_{coil} h_o} + \frac{1}{2\pi k_c L_{coil}} ln\frac{d_o}{d_i} + \frac{1}{\pi d_i L_{coil} h_i}\right)^{-1} \tag{4.14}$$

The outer surface area of heat exchanger, A_o

$$A_o = \pi d_o L_{coil} \tag{4.15}$$

The inner surface area of heat exchanger, A_i

$$A_i = \pi d_i L_{coil} \tag{4.16}$$

The terms, R_t is the total thermal resistance given by the sum of the thermal resistances associated

with the natural convection outside the coil, the conduction across the thickness of the coil tube and the forced convection inside the coil. Likewise, h_o and h_i represent the heat transfer coefficient of the natural and forced convection, respectively, k_c is the thermal conductivity of the copper tube, d_o and d_i are the outer and inner diameter of the coil tube respectively.

4.4.3 Inner Convection Heat Transfer Coefficient

As per Cuiping, et.al [61] the inside coil heat transfer coefficient, h_i, can be expressed in terms of inner Nusselt number correlation of Equation (4.17) as follows [41].

$$Nu_i = 0.0397(Re)^{0.784}(Pr)^{0.3} \tag{4.17}$$

$$h_i = \frac{Nu_i * k_c}{d_i} \tag{4.18}$$

Where, Pr is the Prandtl number.

$$Pr = \frac{C_P * \mu}{k_c} \tag{4.19}$$

In Refs. [41], the critical Reynolds number for helical pipe flow, which determines the flow is laminar or turbulent, is related to the curvature ratio as follows:

$$Re_{cr} = 2300\left[1 + 8.6\left(\frac{d_i}{D_C}\right)^{0.45}\right] \tag{4.20}$$

Calculation of coil curvature ratio, $\delta = \frac{d_i}{D_c}$

$$= \frac{6.78mm}{250\ mm} = 0.02712$$

On substituting the value of, δ into Equation. (4.22)

$$Re_{cr} = 6201.3 > 4000$$

So, according to Equation (4.20) the flow inside the coil tube is turbulent and forced convection.

4.4.4 Outer Convection Heat Transfer Coefficient

Correlation expressed in Eq. (4.21) was established using the tube outer diameter as characteristic length, in order to calculate the outer natural convection heat transfer coefficient as follows [61].

$$Nu_{do} = 0.36 + \frac{0.518 * Ra^{0.25}}{\left[1 + \left(\frac{0.559}{Pr}\right)^{\frac{9}{16}}\right]^{\frac{4}{9}}} \tag{4.21}$$

Terms: Rayleigh number, $Ra = Gr * Pr$ (4.22)

Grashof number, $Gr = \frac{g\beta d_o^3 \Delta T}{\upsilon^2}$ (4.23)

Where, g = Acceleration of gravity = 9.81, m/s^2

β = Coefficient of volumetric thermal expansion

ΔT = Temperature gradient

υ = Kinematic viscosity

Then pipe-outer heat transfer coefficient is calculated from the following equation

$$h_o = \frac{Nu_{do}\, k}{d_o} \quad (4.24)$$

4.5 Energy Balance Equations

The overall energy balance of any two-fluid heat exchanger, satisfying first law of thermodynamic is given by Equation (4.25) [48].

$$Q = UA_o\Delta T_{LMTD} = \dot{m}_w C_p \Delta T \quad (4.25)$$

This implies,

$$Q = \dot{m}_w C_p\left(T_{s,f} - T_{w,r}\right) = UA_o\Delta T_{LMTD} \quad (4.26)$$

Where: $T_{s,f}$ = final hot water temperature inlet to the coil tube

$T_{w,r}$ = water temperature outlet from the coil tube

$\dot{m}_w$ = mass flow rate of water

However, the final hot water temperature inlet to coil or storage tank water temperature supplied to the next loop at any time step can be estimated from the initial storage tank temperature as follows.

$$T_{s,f} = T_{s,i} + \frac{tstep}{\dot{m}_w C_p}\left(\dot{Q}_U - \dot{Q}_{Load} - \dot{Q}_{Loss}\right) \quad (4.27)$$

From equation 4.27, the return water temperature through coil outlet to the solar collector thermal storage, $T_{w,r}$ evaluated as:

$$T_{w,r} = T_{s,f} - \frac{U_o A_o \Delta T_{LMTD}}{\dot{m}_w C_p} \quad (4.28)$$

The log mean temperature in equation (4.29) is also expressed as follows:

$$\Delta T_{LMTD} = \frac{\left(T_{s,f} - T_{m,f}\right) - \left(T_{w,r} - T_{m,i}\right)}{ln\frac{\left(T_{s,f} - T_{m,f}\right)}{\left(T_{w,r} - T_{m,i}\right)}} \quad (4.29)$$

4.5.1 Actual Heat Transfer Rate in a Heat Exchanger

The actual heat transfer rate in a heat exchanger, $\dot{Q}_{act}$ from an energy balance on the hot or cold fluids can be determined from the following equation [67]

$$\dot{Q}_{act} = C_h\left(T_{h,i} - T_{h,o}\right) = C_c(T_{m,f} - T_{m,i}) \quad (4.30)$$

This implies, $m_m C_{p,m}(T_{m,f} - T_{m,i}) = UA_o\Delta T_{LMTD}$

Where, $T_{h,i}$ and $T_{h,o}$ are the hot water temperature inlet to the coil and outlet from the coil respectively. C_h and C_c are also the heat capacity rates of the hot and cold fluids respectively, m_m is the mass of milk, $C_{p,m}$ is specific heat capacity of milk, $T_{m,f}$ and $T_{m,i}$ are final and initial milk temperature respectively.

4.6 Pressure Drop and Pumping Power

4.6.1 Pressure Drop in the Coil Tube

The total pressure drop inside coil tube is the sum of three resistances, such as resistance along the pipe, bending resistance and resistance of the import and export of connecting tubes fittings. [42] [61].

Pressure drop along the Pipe

The resistance along the pipe, ΔP_i is calculated from the following equation:

$$\Delta P_i = \frac{f L_{coil}\rho V_i^2}{2d_i} \quad (4.31)$$

Calculation of friction factor, f using Reynolds Number for turbulent flow inside tube is given by following expresion [65].

$$f = \frac{7.2}{Re_i^{0.5}}\left(\frac{d_i}{D_c}\right)^{0.25} \quad (4.32)$$

Calculation of internal Reynolds Number, Re_i

$$Re_i = \frac{\rho_h V_i d_i}{\mu} \quad (4.33)$$

The terms, ρ_h is hot water density ($990.688 Kgm^{-3}$), μ is the dynamic viscosity (0.00062 N-s/m^2), $d_i = 0.00678m$ and V_i is velocity of hot fluid rate inside the tube assumed to 0.5 m/s [60].

On substituting the values: $Re_i = 5417$ and $f = 0.0397$ into Equation 4.31.

$$\Delta P_i = \frac{0.0397 * 3.5 * 990.688 * 0.5^2}{2 * 0.00678}$$

$$= 2538\ Pa$$

Pressure Drop in Bends

The total pressure drop in a bend is the sum of the frictional head loss due to the length of the bend, head loss due to curvature, and head loss due to excess pressure drop in the downstream pipe because of the velocity profile distortion. Which is calculated by the following equation [42].

$$\Delta P_b = K\frac{\rho {V_i}^2}{2} \tag{4.34}$$

Where, the total loss coefficient, K expressed as:

$$K = \frac{4fL_{coil}}{D_h} + K^* \tag{4.35}$$

Here, K^* the loss coefficient, for turbulent flow the recommended value is given as following:

$$K^* = B(\varphi)\left[0.051 + 0.38\left(\frac{R}{d_i}\right)^{-1}\right] \tag{4.36}$$

Where:

$$B(\varphi) = \begin{cases} 1 & for\ \varphi = 90^0 \\ 0.9sin\varphi & for\ \varphi \le 70^0 \\ 0.7 + 0.35\sin\left(\frac{\varphi}{90}\right) & for\ \varphi \ge 70^0 \end{cases} \tag{4.37}$$

$$D_h = 4\frac{A_c}{P_w} = \frac{4(Net\ free\ flow\ area)}{Wetted\ perimeter} \tag{4.38}$$

Where: f = friction factor for a straight pipe at the Reynolds number in the bend

K^* = combined loss coefficient other than friction loss

Dh = hydraulic diameter for pressure drops, and for circular tube its value equal to coil tube inner diameter, d_i

R = radius of curvature, $(D_c/2)$ see Fig: 2.9

r = coil tube inside radius, m

φ = tube bending angle, in degree

Using, $Re = 5417$, $\varphi = 360^0$, R = 0.125m, $D_h = 0.00678m$ and $f = 0.0397$

Substituting: $B(\varphi) = 0.7 + 0.35\sin(\varphi/90)$ $for\ \varphi \ge 70^0$

$$= 0.7244$$

$$K^* = B(\varphi)\left[0.051 + 0.38\left(\frac{R}{d_i}\right)^{-1}\right]$$

$$= 0.051875$$

Then, total loss coefficient

$$K = \frac{4fL_{coil}}{D_h} + K^* = \frac{4 * 0.0397 * 3.5}{0.00678} + 0.051875$$
$$= 82.03$$

Substituting the above values into Equation (4.41)

$$\Delta P_b = K\frac{\rho {V_i}^2}{2} = 82.03\frac{990.688 * 0.5^2}{2} = 10158.3Pa$$

Pressure Drop in the Fittings

The pressure drop at the import and export connecting tube fitting, is calculated as a total loss coefficient, [61].

$$\Delta P_f = 1.5\frac{\rho V_i^2}{2} \quad (4.39)$$
$$= 185.754\ Pa$$

Then, the total pressure drop in the coil, ΔP is:

$$\Delta P = \Delta P_i + \Delta P_b + \Delta P_f \quad (4.40)$$
$$= 2538 + 10158.3 + 185.754$$
$$= 12882.054 \text{ Pa}$$

This total pressure drop is less than the total allowable value of $0.3 \times 10^5\ Pa$ for helical coil, so this value is **acceptable** [61].

4.6.2 Pressure Drop in Pipe Lines

As shown on Fig :3.3, there are connecting pipe lines in the system, such as from thermal storage outlet to coil inlet and return pipe lines from coil outlet to solar water storage tank. The pressure drop in a pipe, due to friction is a function of the fluid flow-rate, fluid density, viscosity, pipe diameter, pipe surface roughness and the length of the pipe.

It can be calculated using the following equation [68]

$$\Delta P = f\frac{L_p}{d}\frac{1}{2}\rho V^2 \quad (4.41)$$

Where: ΔP = pressure drop, N/m^2

f = Darcy friction factor,

L_p = pipe length, m

d = pipe inside diameter, m

V = fluid velocity, m/s.

The friction factor is dependent on the Reynolds number and pipe roughness, can be found from Moody chart of Fig D.1.

Relative roughness, $\epsilon =$ absolute roughness / pipe inside diameter (4.42)

$$Re = \frac{\rho V d}{\mu} \tag{4.43}$$

Pipe head loss, h_f due to friction is obtained as following:

$$h_f = f\frac{L_p}{d}\frac{V^2}{2g} \tag{4.44}$$

Minor loss, h_L due to piping component

$$h_L = K_L\frac{V^2}{2g} \tag{4.45}$$

Summing Equation (4.44) and (4.45) the total head loss, h_{tot} obtained as follows.

$$h_{tot} = h_f + h_L \tag{4.46}$$

$$= \frac{V^2}{2g}\left(f\frac{L_p}{d} + \sum K_L\right)$$

Where, $K_L =$ Pressure loss factor

Suppose the total closed loop pipe length of supply and return pipe lines to be, $L_p = 4$ m and as shown in Fig: 3.3 there are 4 bends. Then, for 90^0 standard elbow, $K_L = 1.5$, tank entry k = 0.5 tank exit = 1

Properties of water at 50 ^{0}C (suppose average water temperature inside pipe lines) $\rho = 998kg/m^3$, and $\mu = 1.003 \times 10^{-3}\ Kg/m.s$

Where as, $v \leq 2m/s$ was recommended value for pump selection, using $v = 1.8\ m/s$ and 32 mm internal diameter galvanized steel pipe:

Internal area of pipe can be:

$$A_i = \frac{\pi D^2}{4} = \frac{\pi * 0.032^2}{4} = 8.0425 \times 10^{-4} m^2$$

$$Re = \frac{\rho V d}{\mu} = \frac{998 \times 1.8 \times 0.032}{1.003 \times 10^{-3}}$$

$$= 57312.86$$

For galvanized steel the equivalent roughness is ($\epsilon = 0.15mm$)

$$\frac{\epsilon}{d} = 0.0046875$$

Enter the Moody chart on the right at ϵ/d ≈ 0.0047 (with interpolate), and move to the left to intersect with Re ≈ 57313.

Reading of $f \approx 0.03$. Then, the total head loss using Equation (4.46) becomes:

$$\text{Sum of losses, } \sum K_L = (4 * 1.5) + 2 * 0.5 + 1 * 2 = 9$$

$$h_{tot} = \frac{1.8^2}{2 * 9.81}\left(0.03 * \frac{4}{0.032} + 9\right)$$
$$= 2.10\ m$$

Finally, substituting the values into Equation (4.41);

$$\Delta P = f\frac{L_p}{d}\frac{1}{2}\rho V^2$$
$$= 0.03 * \frac{4}{0.032} * \frac{1}{2} * 998 * 1.8^2$$
$$= 6063\ Pa$$

4.6.3 Total Pressure Drop in the System

The total pressure drop in the system is the result sum of pressure drops in Equations (4.40) and (4.41)

$$\Delta P_{tot} = 12\,882.054\ Pa + 6063\ \ Pa \qquad (4.47)$$
$$= 18\,945\ Pa$$

4.6.4 Determination of Total Dynamic Head

- **Total specific work of water pump**

  Total pressure drop, $\Delta P_{tot} = 18\,945 Pa$

  Then, total specific work is given by:

  $$Y = \frac{\Delta P_{tot}}{\rho} = \frac{18\,945\ \text{Pa}}{998\ \text{kg/m}^3} = 18.98\ m^2/\text{s}^2$$

- **Total Head**

  Total Specific Work is ($18.98\ m^2/s^2$); then total dynamic head, H is:

  $$H = \frac{Y}{g} = \frac{18.98}{9.81} \approx 2\ \text{m}$$

4.7 Pumping Power Requirement

The fluid pumping power, P in considering the total system head loss, h_{sys} the input fluid pumping power can calculated using Equation (4.48) [68].

$$P = \frac{\rho . g . Q . h_{sys}}{\eta_m \eta_p} \qquad (4.48)$$

Here, $h_{sys} = h_{tot} + h_Z$ (4.49)

Where, $h_Z =$ head loss of pump due to elevation, let take it 1.5 m.

$Q_v = VA_i$ is volume flow rate, m^3/s and

η_p is the pump efficiency $(\eta_p = 0.80 - 0.85)$ using 0.80

Substituting:

$$h_{sys} = 2.10 + 1.5 = 3.6\,m$$

$$Q_v = 1.8 \times 8.0425 \times 10^{-4}$$

$$= 1.45 \times 10^{-3} m^3/s$$

Allowing for motor efficiency, $\eta_m = 0.9$

$$P = \frac{\rho . g . Q_v . h_{sys}}{\eta_m \eta_p}$$

$$= \frac{998 \times 9.81 \times 1.45 \times 10^{-3} m^3 \times 3.6}{0.8 \times 0.9}$$

$$= 70.98\,W$$

Therefore, power requirement for PV array ≈ 71 Watt

4.7.1 Pump selection

Active water circulation system is selected to complete the solar milk pasteurizer system considered. Solar powered water pumps are designed to use the direct current (DC) provided by a photovoltaic (PV) array.

However, determination of specific pump size and PV array is based on the performance charts provided by the manufacturers refering to pumping power, total dynamic head and desired pumping flow rate as shown in Fig D.3 (Kyocera Solar pump manufacturer,Inc catalog).

The PV array will be specified in terms of wattage and voltage. It is standard procedure to increase the specified wattage by 25% (multiply by 1.25) to compensate for power losses due to high heat, dust, aging, etc. Therefore, total amount of power needed for pumping by the solar panel was approximately 90 Watt.

CHAPTER FIVE

RESULTS AND DISCUSSIONS

In this chapter, design results and simulation results from a MATLAB code developed under Appendix A-1 for small-scale milk pasteurization system studied are generated graphically and discussed to analysis the performance of the overall system mentioned in Chapter 1.

5.1 Design Results

Table 5.1 shows designed coil heat exchanger geometrical values.

Table 5.1: Coil heat exchanger design parameter values

Parameter	Value	Unit
Outer tube diameter of coil, d_o	8	mm
Inner tube diameter of coil, d_i	6.78	mm
Thickness of tube, t	0.61	mm
Coil diameter, D_C	250	mm
Coil length, L_{coil}	3.5	m
Number of coils turns, N_{coil}	5	-
Total heat transfer area, A_o	0.081	m^2

In addition, the total pressure drop inside the coil was about 12.88KPa which is less than the total allowable value of 30KPa for helical coil heat exchanger [61] and acceptable. However, the total pressure drops of the overall system in considering the pipe line pressure losses and the pumping power requirements are 18.9 KPa and 90 W respectively. The total volume of milk storage tank after the volume occupied by the coil heat exchanger was 0.11 m^3 or 110 liters with internal height of 800 mm and 420 mm diameter.

5.2 Simulation Results

5.2.1 Monthly Average Solar Radiation on Inclined Surface

The simulation begins with estimation of the solar energy potential of the study location. Fig: 5.1 shows the monthly average hourly solar radiation on inclined surface in Watt per meter square for each average months of the year. As shown in the figure, the variation of solar energy on inclined surface at 26.1^0 was between 480 W/m^2 to 920 W/m^2 at the solar noon.

However, the variation of solar energy for each month of the year was due to sunshine hour duration, ambient temperature and solar radiation varies on the earth's surface throughout the year.

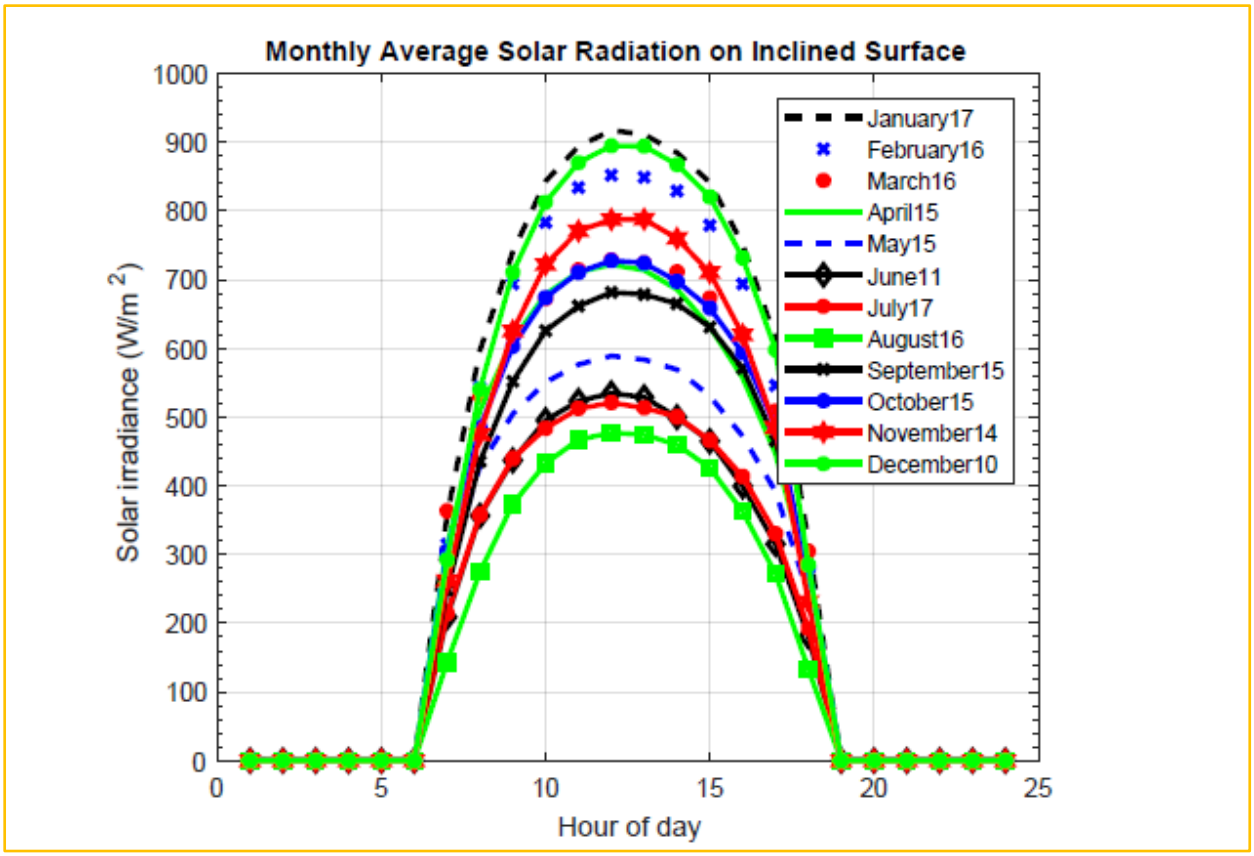

Figure 5.1: Monthly Average Solar radiation on inclined surface, Kombolcha

5.2.2 Monthly Average Hourly Useful Energy

The simulated solar energy on inclined surface of a collector was an input for the useful heat energy generated by the absorber plate and for the outlet hot water exit from the collector. Meanwhile, the values are also depending on glass temperature (Fig 5.2) and ambient temperature for each month of the year as shown in Fig: 5.3 with addition to solar collector size.

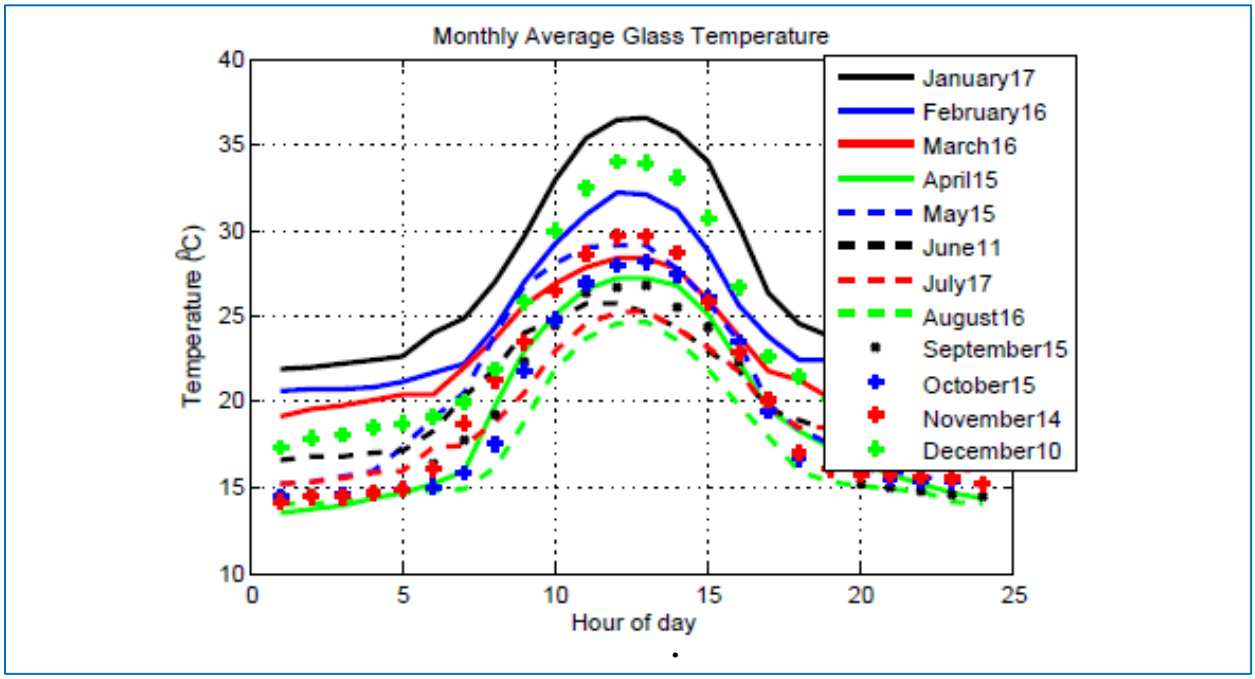

Figure 5.2: Monthly average glass temperature

The useful solar energy transferred through the aluminum fin and the wall of the U-type copper tube to the working fluid was an effective energy gained ($\dot{Q}_u$), and this solar useful energy for each average month of the year in Watt hour for 24-hour simulation period was shown in Fig 5.3.

As seen in the figure, it is clearly observed that the useful heat energy attains its maximum value at the same time, when the solar irradiance was maximum. From the figure, the lowest curve indicates 780-Watt hour useful heat gained in month August and the peak was 1500-Watt hour in month January with 2.11 m^2 gross area of an evacuated tube solar collector.

However, atmospheric condition has a great impact on useful energy gained by the solar collector and its performance also depends considerably by collector size and the solar energy availability at the time being.

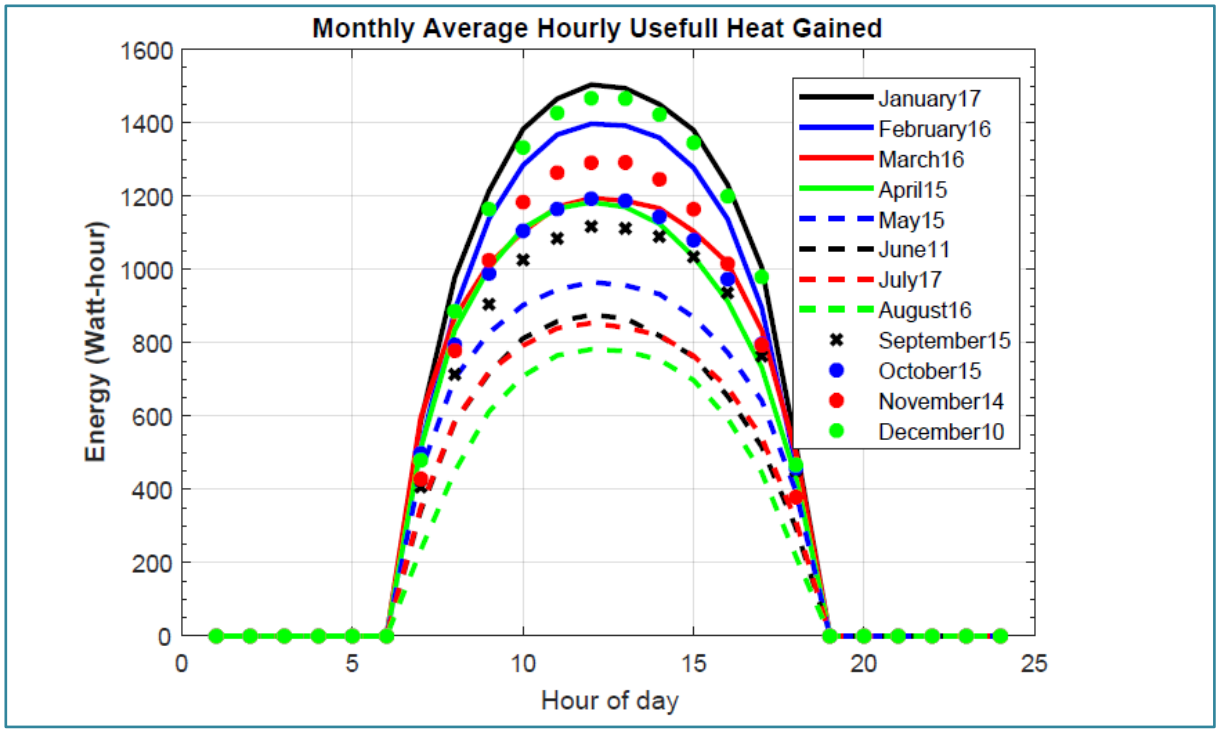

Figure 5.3: Monthly average hourly useful energy

5.2.3 Monthly Average Hot Water Temperature Exit from the Collector

Fig: 5.4 shows the hot water temperature exit profile from the solar collector tubes and accumulated into the horizontal thermal storage tank based on thermosiphon principle of Fig 2.3 which finally utilizes the immersed coil heat exchanger for milk pasteurization process.

Results presented in the figure, shows the daily hot water temperature profile for each month of the year simulated from an initial water temperature of 20^0C considered versus hour of the day. During day time as the sunrises, the trends show that there is an increase of water temperature inside each U-pipe evacuated tubes from 20 ^{0}C to its maximum value at about active solar period (12.00 – 13.30 o'clock) and inversely declined till to 18.00 PM.

This is due to the system operates during sunlight hours, so it is worth to observe that the hot water temperature exits from the collector switched off at 18.00 PM. After that, the water temperature remains constant (during evening) was indicate the water temperature in the thermal storage tank after heat loss to the ambient.

From figure it can be seen also, the lowest curve indicates the average minimum outlet water temperature 80 ^{0}C (August), and maximum 83.42 ^{0}C of January exit water temperature from the collector and at the same time inlet to a fully stratified thermal storage tank studied. However, the outlet water temperature depends upon the solar radiation and Number of tubes.

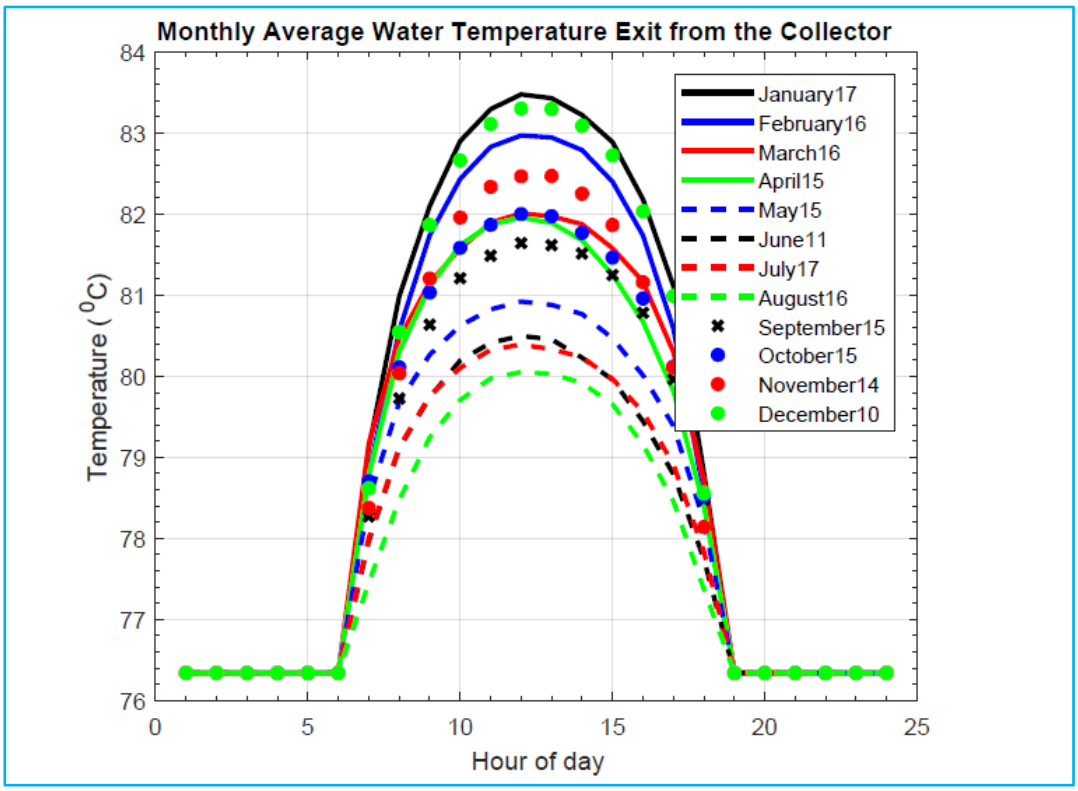

Figure 5.4: Monthly average hourly hot water temperature

5.2.4 Monthly Average Thermal Storage Tank Water Temperature

In similar manner, Fig 5.5 shows the thermal storage tank hot water temperature profile inlet to an immersed coil heat exchanger. However, variation of heat transfer fluid temperature in the storage tank as operation started after energy losses clearly shown in figure for each average months of the year.

As shown, while the cold milk heated by the heat transfer fluid initially there is a slightly decrease in temperature seen in the thermal storage tank at about 10 AM that is the time when pasteurization will be started as shown in Fig.5.6.

Indeed, from about 10:00 AM after energy balance attained the heat transfer fluid temperature in the inlet section of coil undergo a strong increase proportional to the thermal storage tank water

temperature rise as the solar radiation increases. And, for each average month of the year the maximum value of the heat transfer fluid temperature was get its maximum value at about 16.00 PM. After that, the temperature begins to decline because of heat losses from storage tank and drops of solar radiation and decreases in ambient temperature values.

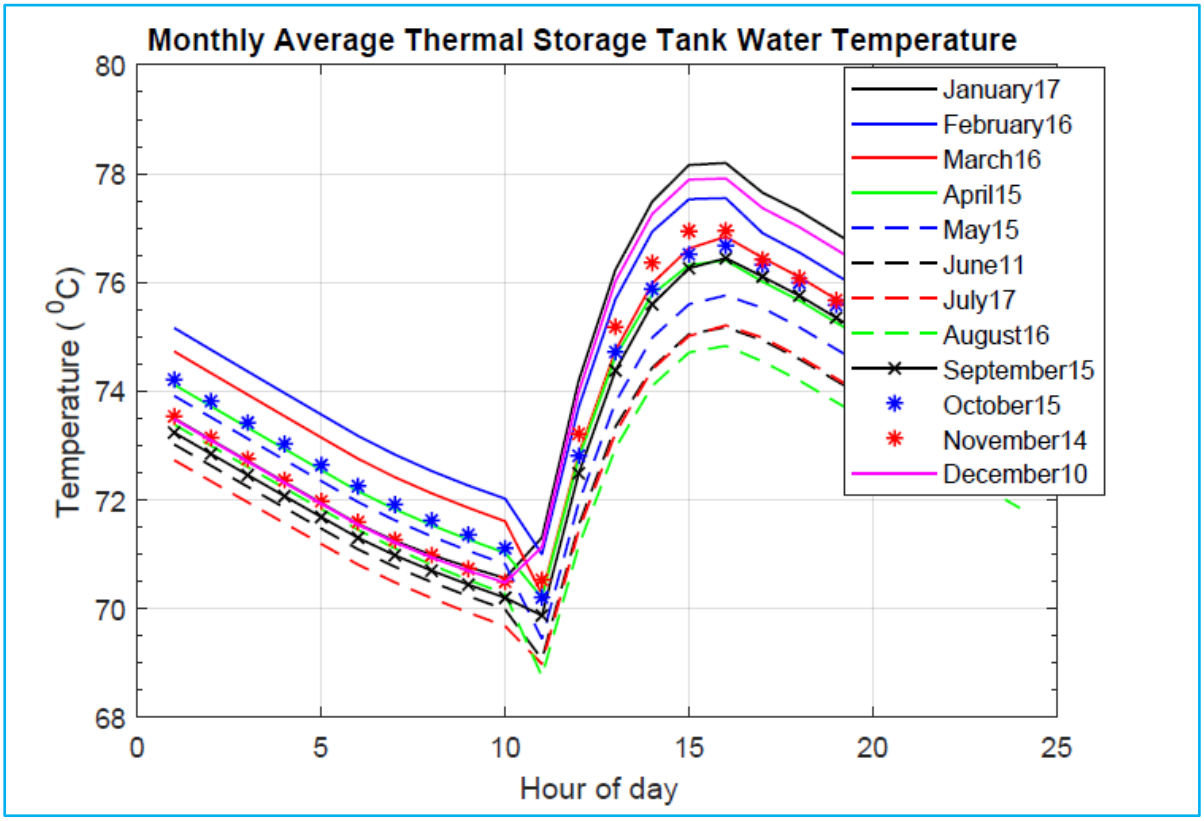

Figure 5.5: Monthly average thermal storage tank temperature

5.2.5 Pasteurized Milk Temperature

For simulation of pasteurized milk temperature, the logarithmic mean temperature difference method was performed between the cold milk and the hot water inlet through the coil heat exchanger from thermal storage tank.

Fig 5.6 illustrate the variation of heated milk temperature versus hour of the day for each average months of the year set being started at about 10 AM. The average monthly pasteurized milk temperature, heated by the hot water fluid flowing through the coil heat exchanger as loading energy for heating raw milk was reaches 65.0 to 69.2 ^{0}C from the initial milk temperature of 32 ^{0}C at about 16 PM.

Afterward, the pasteurized milk temperature declines slightly and remain constant in milk storage tank after heat losses through the tank wall. However, this milk temperature value is within the acceptable range of being milk heated to achieve batch type pasteurization temperature requirement of 63 ^{0}C to 72 ^{0}C [14] [23].

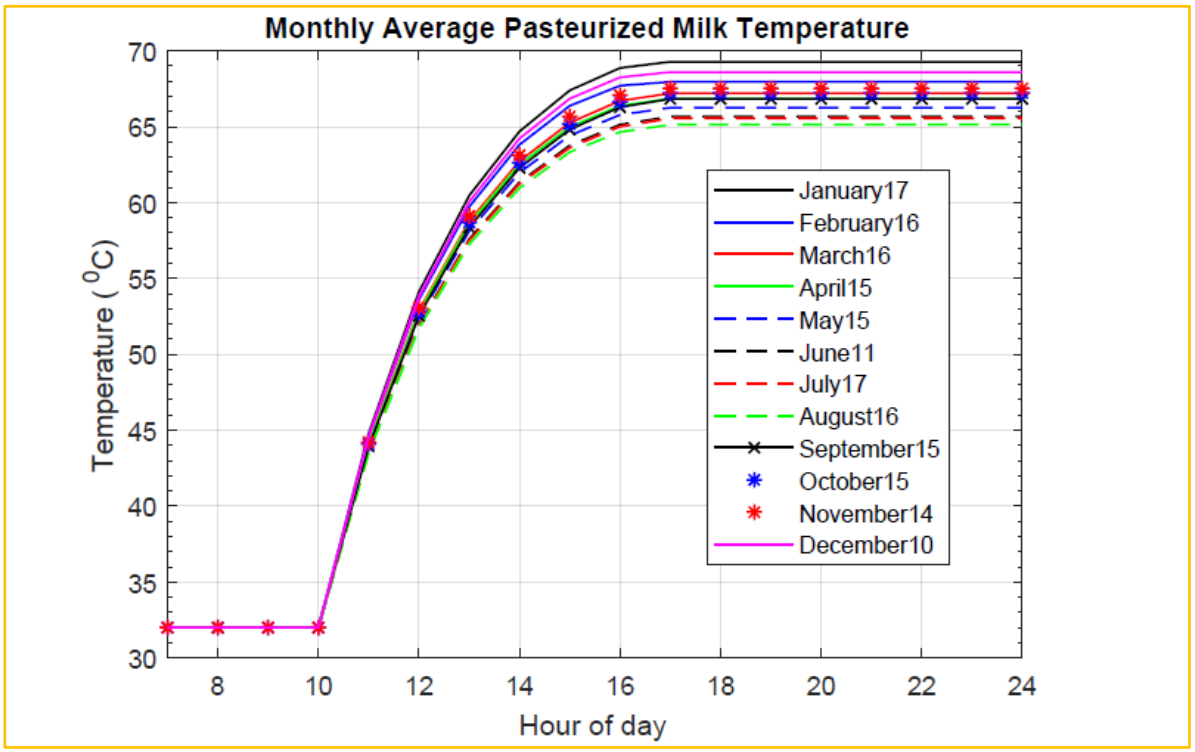

Figure 5.6: Monthly average pasteurized milk temperature

MATLAB environment was used by many engineers and researchers around the world to validate solar water heating system and obtained a good and accurate result as compared to experimental values measured at the same condition.

As reviewed in section 2.9, some researchers conduct experiment to pasteurize milk using solar energy in different way as this study. It is clearly observed that, the quantity of milk being heated was a direct impact on the pasteurized milk temperature.

Wayua, et.al [49] obtained 81.4 ^{0}C for 20 lt/day and 41.7 ^{0}C for 70 lt/day of pasteurized milk temperature using hot water jacketed milk heating system experimentally. And also, Atia, et.al [11] for selective months of the year attained 63^{0}C for 73.9 lt/day and 72^{0}C for 37.3 lt/day pasteurized milk temperature though heating the raw milk directly with flat plate collector as the working fluid.

As seen in Fig 5.6, from performance analysis of pasteurizing 100 liter of milk per day a recommended milk temperature was achieved due to coil heat exchanger. For comparison, the minimum pasteurized milk temperature was 65. 0 ^{0}C, August 16 and the maximum were 69.2 ^{0}C for January 16. Therefore, the result obtained from the considered model was moreover effective in contrast to the above researchers using mechanism to pasteurize milk even though the study was not conducted or tested experimentally.

CHAPTER SIX

CONCLUSIONS AND RECOMMENDATIONS

6.1 Conclusions

In this paper, a small-scale milk pasteurization system was developed using solar energy and the model performance analysis was done with a MATLAB code. From simulation results, the hourly monthly solar energy on inclined surface of the study location were between 480 to 920 W/m^2. The average monthly useful energy gained with a 2.11m^2 gross area of an evacuated tube solar collector inclined at 26.1^0 and using water as working fluid was varies between 780Wh to 1500 Wh for each average month of the year.

The hourly trends of the hot water temperature exit from the collector and stored into a thermal storage tank for each average month of the year was also 80 to 83.42 ^{0}C. However, the hot water temperature in the thermal storage tank or inlet to the coil heat exchanger after energy loss to the ambient was between 69.0^{0}C to 78.2 ^{0}C. Moreover, the average monthly pasteurized milk temperature obtained from the system analysis were between 65.0 to 69.2 ^{0}C and these values are within acceptable standard temperature range of milk being pasteurized.

However, accuracy of meteorological data and lack of continuity are the main impact while analysis solar energy of the location. Finally, it is concluded that utilizing freely available source solar energy in this manner to destroy microorganisms that leads milk easily spoils was attractive.

6.2 Recommendations

This study revealed that, it is possible to pasteurize liquid milk by using solar thermal energy for Kombolcha town with acceptable milk pasteurized temperature. However, the following points are recommended for further investigation on the studied model.

- Experimental investigation was suggested to test the only modelled system performance to get an accurate practical configuration.
- Optimizing the model performance processing or heating time of milk pasteurization with motor driven agitator.
- Cost estimation of the overall system for future commercialization.
- Optimizing the model for large scale application with backup hot water storage tank and its supply system.

REFERENCES

[1] Neijenhuis, F., "Possible Interventions in Butter & Liquid Milk Processing by the EDGET project,Addis Ababa, Ethiopia," Wageningen UR Livestock Research, 2014.

[2] Vassilios, R., "Effect of heat treatment on milk protein functionality at emulsion interfaces. A review," Food Hydrocolloids, vol. 24, p. 259 – 265, 2010.

[3] Yildirim,N., Genc,S., "Energy and exergy analysis of a milk powder production system," Energy Conversion and Management, vol. 149, p. 698 –705, 2017.

[4] Tadesse, G. and Mengistie, A., "Challenges, Opportunities and Prospects of Dairy Farming in Ethiopia: A Review," World Journal of Dairy & Food Sciences, vol. 11, no. 1, pp. 01 - 09, 2016.

[5] Tadesse, M., Fentahun, M., Tadesse, G., "Dairy Farming and its Economic Importance in Ethiopia: A Review," World Journal of Dairy & Food Sciences, vol. 12, no. 1, pp. 42 - 51, 2017.

[6] Steen,M. and Maijer,W., "Inclusiveness of the Small - Holder Farmer Key Success Factors for Ethiopian Agribusiness Development," International Food and Agribusiness Management Review, vol. 17, no. B, pp. 83 - 88, 2014.

[7] Tegegne, A., Gebremedhin, B., Hoekstra, D., Belay, B. and Mekasha, Y., "Smallholder dairy production and marketing systems in Ethiopia: IPMS experiences and opportunities for market-oriented development," in Project Working Paper 31, Nairobi, 2013.

[8] Land O'Lakes, "The Next Stage in Dairy Development for Ethiopia Dairy Value Chains, End Markets and Food Security," Addis Ababa, Ethiopia, 2010.

[9] Habtamu, R.L., R. Singh and Kaur,N. , "Determinants of supply chain coordination of milk and dairy industries in Ethiopia: A case of Addis Ababa and its surrounding," Springer Open Journal, vol. 4, no. 498, pp. 1287-1299, 2015.

[10] Kassahun A., Berhan T. and Ashenafi M., "Cattle Fattening System and its Structure in Urban and Peri-Urban Kebeles of Dessie and Kombolcha Towns, Ethiopia," World Applied Sciences Journal , vol. 35, no. 1, pp. 10-17, 2017.

[11] Atia, M. F.; Mostafa, M. M.; Abdel-Salam, M. F.; El-Nono, and M. A., "Solar Energy Utilization for Milk Pasteurization," Solar Energy Systems, pp. 1 -15, 2015.

[12] Yildirim,N. and Genc, S., "Thermodynamic analysis of a milk pasteurization process assisted by geothermal energy," Energy, pp. 987- 996, 2015.

[13] Modi. A., Prajapat R., "Pasteurization Process Energy Optimization for a Milk Dairy Plant by Energy Audit Approach," International Journal of Scientific & Technology Research, vol. 3, no. 6, pp. 181 - 188, 2014.

[14] Patel, R., Patel, A. D., Upadhyay, J. B., "Use of Renewable Energy in Dairy Industry," International Journal of Advance Research and Innovation, vol. 4, no. 2, pp. 433-437, 2016.

[15] Yodit, A., Fanta, D., Bedaso,M., Robel, G., Takele, B., Tariku,J., Fanos, T., Mesula, G. and Ashenafi, F., "Assessment of Staphylococcus aureus along milk value chain and its public health importance in Sebeta, central Oromia, Ethiopia," BMC Microbiology, vol. 17, p. 141, 2017.

[16] Bereda, A., Yilma Z. and Nurfeta, A., "Handling, processing and utilization of milk and milk products in Ezha district of the Gurage zone, Southern Ethiopia," Journal of Agricultural & Biological sustainable development , pp. 91-98, 2013.

[17] Makita, K., Desissa, F., Teklu, A., Zewde, G., Grace, D., "Risk assessment of staphylococcal poisoning due to consumption of informally marketed milk and home-made yoghurt in Debre Zeit," International Journal of Food Microbiol., vol. 1, no. 2, pp. 135 - 153, 2012.

[18] Ruangwittayanusorna,K. , Promketa,D., Chantiratikula,A. , "Monitoring the Hygiene of Raw Milk from Farms to Milk Retailers," Agriculture and Agricultural Science Procedia, vol. 11, p. 95 – 99, 2016.

[19] Yilma, Z., Guernebleich, E., Ameha,S., "A Review of the Ethiopian Dairy Sector," Food and Agriculture Organization of the United Nations, Sub Regional Office for Eastern Africa, p. 81, 2011.

[20] Flores-Flores,M. E., Lizarraga,E. De Cerain,A. L., Penas,E. G. , "Presence of mycotoxins in animal milk: A review," Food Control, vol. 53, pp. 163 - 176, 2015.

[21] Demissu, H., "Assessment on Peri-Urban Dairy Production System and Evaluation of Quality of Cows' Raw Milk: A Case of Shambu, Fincha and Kombolcha Towns of Horro Guduru Wollega Zone, Ethiopia," Science, Technology and Arts Research Journal, vol. 3, no. 3, pp. 37 -43, 2014.

[22] Karunasree,P., "Review - A Brief Study on Milk," Journal of Food and Dairy Technology, vol. 4, no. 3, pp. 2347- 2359, 2016.

[23] Simran Watts, "A mini review on technique of milk pasteurization," Journal of Pharmacognosy and Phytochemistry , vol. 5, no. 5, pp. 99-101, 2016.

[24] Farjana,S.H., Huda, N., Parvez, M., Saidur,R. , "Solar process heat in industrial systems – A global review," Renewable and Sustainable Energy Reviews, pp. 1 - 17, 2017.

[25] Jamar,A. ,Majid, Z.A., Azmi,W.H., Norhafana,M., Razak,A., "A review of water heating system for solar energy applications," International Communications in Heat and Mass Transfer, vol. 76, pp. 178 - 187, 2016.

[26] Sharma,A., Sharma,C., Subhash,C., Mullick,C., Kandpal,T., "Solar industrial process heating: A review," Renewable and Sustainable Energy Reviews, vol. 78, p. 124–137, 2017.

[27] Fathima, A., Sreekala, P., Mathew,B., "Performance Analysis of Solar Thermal Evacuated Tube Collector Using Different nano fluids," International Journal of Engineering Sciences & Research Technology, vol. 5, no. 7, pp. 367 - 373, 2016.

[28] Sadhishkumar, S., Balusamy, T., "Performance improvement in solar water heating Systems a review," Renew Sustain Energy, vol. 37, pp. 191 -8, 2014.

[29] Deepak, D., Raol,J., Sunil,P., Chauhan,I., "Application of Solar energy for sustainable Dairy Development," European Journal of Sustainable Development, vol. 2, no. 4, pp. 131 - 140, 2013.

[30] Wang,Z., Yang,W., Feng Qiu, Zhang,X., Zhao,X. , "Solar water heating: From theory, application, marketing and research," Renewable and Sustainable Energy Reviews, vol. 41, p. 68 – 84, 2015.

[31] Gao,Y., Fan,R., Zhang,X.Y., AN,Y.J., Wang,M.X., Gao,Y.K., Yu, Y., "Thermal performance and parameter analysis of a U-pipe evacuated solar tube collector," Solar Energy, vol. 107, pp. 714 - 727, 2014.

[32] Ghoneim,A., "Optimization of Evacuated Tube Collector Parameters for Solar Industrial Process Heat," International Journal of Energy and Environmental Research, vol. 5, no. 2, pp. 55-73, 2017.

[33] Sabiha,M.A., Saidur,R., SaadMekhilef, OmidMahian, "Progress and latest developments of evacuated tube solar collectors," Renewable and Sustainable Energy Reviews, vol. 51, pp. 1038 -1054, 2015.

[34] Yadav,M., Saikhedkar,N.K., "Simulation Modelling for the Performance of Evacuated Tube Solar Collector," International Journal of Innovative Research in Science, Engineering and Technology, vol. 6, no. 4, pp. 5634 - 5642, 2017.

[35] Aboulmagd,A., Padovan,A., De C.Oliveski,R., Del Col,D., "A New Model for the Analysis of Performance in Evacuated Tube Solar Collectors," in International High Performance Buildings Conference, Purdue University, 2014.

[36] Gao,Y., Zhang,Q., Rui Fan, Lin,X., Yong,Y., "Effects of thermal mass and flow rate on forced-circulation solar hot-water system: Comparison of water-in-glass and U-pipe evacuated-tube solar collectors," Solar Energy, vol. 98, pp. 290 - 301, 2013.

[37] Siva Kumara,S., Mohan Kumar,K., Sanjeev Kumar,S. R. , "Design of Evacuated Tube Solar Collector with Heat Pipe," Materials Today, vol. 4, p. 12641–12646, 2017.

[38] Jafarkazemi,F., Ahmadifard,E., Abdi,H., "Energy and Exergy Efficiency of Heat Pipe Evacuated Tube Solar Collectors," Thermal Science: Year 2016, Vol. 20, No. 1, pp. 327-335, vol. 20, no. 1, pp. 327 -335, 2016.

[39] Suresh, N.S., Badri, Rao,S., "Solar energy for process heating: A case study of select Indian," Journal of Cleaner Production, vol. 151, pp. 439 - 451, 2017.

[40] Panchal,H., Pateland,R., Parmar,D. , "Application of solar energy for milk pasteurisation: a comprehensive review for sustainable development," International Journal of Ambient Energy, pp. 1 - 5, 2018.

[41] Vishvakarma,S., Kumbhare,S., Thakur,K. K. , "A Review on Heat Transfer through Helical Coil Heat Exchangers," International Journal of Engineering Sciences & Research, vol. 8, no. 5, pp. 607 - 612, 2016.

[42] Sadic, K., Hongtan Liu, Heat exchangers, Selection, Rating, and Thermal Design, 2nd ed., Departement of Mechanical Engineering, University of Miami, Florida: CRC press LLC, 2002.

[43] Purandare,P.S., Mandar, M., Lele, Gupta,R.K., "Investigation on thermal analysis of conical coil heat exchanger," International Journal of Heat and Mass Transfer, vol. 90, pp. 1188 - 1196, 2015.

[44] Huang,K., Julie, M., Goddard, "Influence of fluid milk product composition on fouling and cleaning of Ni–PTFE modified stainless steel heat exchanger surfaces," Journal of Food Engineering, vol. 158, pp. 22 -29, 2015.

[45] Shuhong, L., Zhang,Y., Zhanga,K., Li,X., Yang Li, Zhang,X. , "Study on performance of storage tanks in solar water heater system in charge and discharge progress," Energy Procedia, vol. 48, p. 384 – 393, 2014.

[46] Fernández-Seara, J., Diz, R., Uhía, F.J., Sieres, J., Dopazo, J.A., "Thermal Analysis of a Helically Coiled Tube in a Domestic Hot Water Storage Tank," in International Conference on Heat Transfer, Fluid Mechanics and Thermodynamics, Sun City, South Africa, 2007.

[47] Lazova,M., Huisseune,H., Kaya, A., Lecompte,S.,Kosmadakis, G., "Performance Evaluation of a Helical Coil Heat Exchanger Working under Supercritical Conditions in a Solar Organic Rankine Cycle Installation," Energies, vol. 9, p. 432, 2016.

[48] Kuppan,T., Heat Exchanger Design Hand Book, Southern Railway Madras, India: Marcel Dekker, Inc. New York Basel, 2000.

[49] Wayua,F. O., Okoth,M., Wangoh,J. , "Design and Performance Assessment of a Flat- Plate Solar Milk Pasteurizer for Arod Pastoral Areas of Kenya," Journal of Food Processing and Preservation, pp. 1 - 6, 2012.

[50] Azimi, M., Irjavadi, S.S., Mohammadkarim, A., "Simulation and Optimization of Vacuum Tube Solar Collector Water Heating System in Iran," Journal of Science and Engineering, vol. 07, no. 01, pp. 001 - 019, 2016.

[51] Momale, V.C., Yadav, M.S., Pande, S.S., Borse, Y.V., "Analysis of Heat Transfer Coefficients for Helical Coil Heat Exchanger," International Journal on Theoretical and Applied Research in Mechanical Engineering, vol. 6, no. 1 -2, pp. 166 -169, 2017.

[52] Duffie,J.A., Beckman,W.A. , Solar Engineering of Thermal Processes, 4th ed., John Wiley & Sons, Inc.,, 2013.

[53] Adisu, B., Demiss Alemu, Mishrac, M. , "Large Scale Solar Water Heating Systems Analysis in Ethiopia: A Case Study," International Journal of Sustainable Energy, pp. 1 - 41, 2013.

[54] Hafez, A.Z., Soliman, A., El-Metwally, K.A., Ismail, I.M. , "Tilt and azimuth angles in solar energy applications – A review," Renewable and Sustainable Energy Reviews, vol. 77, pp. 147 - 168, 2017.

[55] Reicosky,D.C., Winkelman, L.J., Baker,J.M., Baker,D., "Accuracy of Hourly Air Temperatures Calculated form Daily Minima and Maxima," Agricultural and Forest Meteorology,, vol. 46, pp. 193 - 209.

[56] Praene,J.P., Garde,F., Lucas,F. , "Dynamic Modelling and Elements of Validation of Solar," in Ninth International IBPSA Conference, Montréal, Canada, 2005.

[57] Allouhia,A., Agrouaz,Y., Amine, M.B. , "Design optimization of a multi-temperature solar thermal heating system for an industrial process," Applied Energy, vol. 206, pp. 382 - 392, 2017.

[58] Rodríguez,G.M., Fuentes-Silva,A.L., Núnez,M.P., "Solar thermal networks operating with evacuated-tube collectors," Energy, vol. xxx, pp. 1 - 8, 2017.

[59] Abdul, J.N., Khalifa, Mustafa,A., Farhan,A., Khammas, "Experimental Study of Temperature Stratification in A Thermal Storage Tank in The Static Mode for Different Aspect Ratios," ARPN Journal of Engineering and Applied Sciences, vol. 6, no. 2, pp. 53 - 60, 2011.

[60] Verechshagin,O., Yesseyeva,G., Mukasheva,T., "Methodology to calculate Design Parameters of Screw Heat Exchanger for Vat Pasteurizer," Journal of Engineering and Applied Science, vol. 11, no. 1, pp. 2955 - 2961, 2016.

[61] Cuiping, L., Duanlian, H., Jianqing, D., "Design of Coil Heat Exchanger for Remote-Storage Solar Water Heating System," Solar Energy and Human Settlement, pp. 2123 - 2127, 2007.

[62] Sinnott, R. K., Chemical Engineering Design, Fourth ed., vol. 6, Departement in Oxford, UK: Elsevier, 2005.

[63] Dewangan. AK., Patel, AD., Bhadania, AG., "Stainless Steel for Dairy and Food Industry: A Review," Journal of Material Sciences & Engineering, vol. 4, no. 5, pp. 2169 - 0022, 2015.

[64] Sahu,D.K., Sen,P.K., Sahu,G., Sharma,R., Bohidar,S. , "A Review on Thermal Insulation and Its Optimum Thickness to Reduce Heat Loss," International Journal for Innovative Research in Science & Technology, vol. 2, no. 06, pp. 2349 - 6010, 2015.

[65] Amitkumar,S., Puttewar, Andhare,A.M. , "Design and Thermal Evaluation of Shell and Helical Coil Heat Exchanger," International Journal of Research in Engineering and Technology, vol. 04, no. 01, pp. 416 - 423, 2015.

[66] Mohapatra,T., Padhi,B.N., Sahoo,S.S., Pramanika,R.N., "Performance analysis of three fluid heat exchanger used in solar flat plate collector system," Energy Procedia, vol. 109, pp. 322 - 330, 2017.

[67] Andrzejczyk, R., Muszynski, T., "Performance analyses of helical coil heat exchangers. The effect of external coil surface modification on heat exchanger effectiveness," Thermodynamics, vol. 37, no. 4, p. 137–159, 2016.

[68] Frank M. White, Fluid Mechanics, Fourth Edition ed., University of Rhode Island: McGraw-Hill Series in Mechanical Engineering.

APPENDIXES

Appendix A: MATLAB CODE for Global and Diffuse Radiation

```
z = 1857;                       % elevation of the site above sea level
A= 11.084;                      % latitude of the location
phi= 3.14;
e = 1.367;                      %solar constant
u = 8.242;
c = 'January';                  % sunshine hour
f=xlsread(c);
g=f(1,:);
n=1:31;
%wes = [85.71, 87.41, 89.53, 91.86, 93.82, 94.79, 94.36, 92.69, 90.43, 88.10,
86.15, 85.23];
decl = -20.9;                  % declinatiin angle
   ws = 85.71;                 % hour angle
 Td = 2/15*ws;
  a = -0.309 + 0.539*cos(A)-0.0693*(z)+ 0.290*(u/Td);
  r = 1.449-0.553*cos(A)- 0.694*(u/Td);
  for n=1:30
  Ho =
(24*e/phi)*(1+0.03*cos(360.*n/365)*(cos(A)*cos(decl)*sin(ws)+(phi*ws/180)*sin
(A)*sin(decl)));
  H = Ho*(a+r*(g/Td));
  kt=H/Ho;
  Hd=1.311-3.022*kt+3.427*kt.^2-1.82*kt.^3;
  end
```

Published with MATLAB® R2017a

Appendix B: MATLAB CODE of Main Program

% Hourly Temperature variation of the useful heat, collector, hot water, pasteurized milk and coefficient of performance using the Global Radiation, Diffuse Radiation and ambient temperature % variation data

```
clear all
clc
Ac = 2.11;                  %collector area
Aabs = 1.64;                %collector absorber area
eg=0.88;                    %Emissivity of outer glass
ep = 0.10;                  %Emissivity of plate
ks = 0.024;                 %thermal conductivity of insulator
t = 0.10;                   %Thickness of Insulation of Tank
KAl= 220 ;           %thermal conductivity of aluminum fin
ag =0.94 ;           %absorption coefficient of the selective coating
tg =0.96;            %transmissivity of glass
cp = 4187;           %specific heat of water
Rf = 0.6;            %ground reflectivity
ca = 377;            %heat capacity of absorber plate /copper
cg = 830;            %heat capacity of outer glass
Vw = 2.5;            %wind speed
m = 56;              %mass of water in collector tube
s =5.67e-8;          %Stefan-Boltzmann Constant
kw =0.625;           %Thermal Conductivity of Water
Vs=0.15 ;            %Volume of water storage tank m3
As= 1.98;            %heat transfer area of storage tank
tstep= 60;           %time step
Rhow=998;            %Density of Water
Ti= 20;              %inlet water temperature
Tai =25;             %average ambient temperature
Tgi=28;              %initial outer glass temperature
Tpi= 56;             %initial plate temperature
Tig=Tpi;             %inner glass temperature
Tfi =53;             %initial water exit from evacuated tube
To=25;               %Temperature of Outlet Water
Tso=To;              %initial instantaneous Temperature of Tanker
dgo =0.058;          %diameter of the outer glass tube
dgi = 0.047;         %diameter of the inner glass tube
dAlo=0.01525;        %diameter of the outer aluminum fin
dAli=0.015;          %diameter of the inner aluminum fin
dcuo=0.01;           %diameter of the outer copper tube
dcui=0.0095;         %diameter of the inner copper tube
L=1.5;               %overall length of absorber tube and aluminum fin
Aog = 2.2148;        %area of outer glass tube
Aig = 1.7436;        %area of inner glass tube
mdot = 0.03;         %mass flowrate of water
phii =11.084*pi/180; % latitude
beta = pi/180;        % Collector slope
Vms = 0.1;            % volume of milk storage tank(m^3)
cppm = 3930;          % specific heat of milk
pr1 = 2.99;           % Prandtl number for inside
```

```
pr2 = 4.83;           % Prandtl number for outside
Re = 6201;            % Reynolds number
lc = 3.5;             % length of coil
Gr = 6452.18;         % Grashof number
k1 = 0.654;           % thermal conductivity water
k2 = 0.623;
kc = 385;             % thermal conductivity of the copper tube
Ao = 0.081;           % coil heat transfer
ri = 0.0034;          % coil inner radius
ro = 0.004;           % coil outer radius
mst = 150;            % mass of water
mm = 103;             % mass of milk in the tank
Tmilkin = 32;         % initial milk temperature
n = xlsread('KTD.xlsx');
for j=1:365
data1(:,:,j)=n(j+(23*(j-1)):j*24,:); %Data given for the global radiation,
diffuse radiation and ambient temperature.
end
for n=1:365
decl(n)=(pi/180)*(23.45*sin((2*pi/365)*(284+n))); % declination angle )))
end
for ii=1:24
omega(ii)=(ii-12)*pi/12; % hour angle for each hour of the day. )))
end
% This approximate the plate, glass, and exit temperature for Jan.01 at 1:00AM.
for i=1
GRR=data1(:,1,i);
DRR=data1(:,2,i);
ATT=data1(:,3,i);
for j=1
GR=GRR(1);
DR=DRR(1);
AT=ATT(1);
%The ratio of beam radiation on the tilted surface
Rb=((cos(phiibeta))*cos(decl(i))*cos(omega(j))+sin(decl(i))*(sin(phii-
beta)))/(cos(phii)*cos(decl(i))*cos(omega(j))+(sin(decl(i))*sin(phii)));
if Rb<0
Rb=0;
end
It=Rb*(GR-DR)+(DR*0.5*(1+cos(beta)))+(0.5*Rf*((1-cos(beta))*GR));
In=It*ag;              %solar Energy absorbed by inclined
Tsky = AT- 6;          %sky temperature of the selected site
hp_g_rad   =   (ep-eg)*s*((Tpi^4-Tgi^4)/(Tpi-Tgi));   %radiation   transfer
coefficient between the absorber plate and outer glass
hp_g = hp_g_rad;
hw=5.7+3.8*Vw; %convection heat transfer coefficient around the outer glass
tube
hg_a_rad=eg*s*(((Tgi).^4)-((Tsky).^4))/(Tgi-Tsky);  %radiation  heat  transfer
coeffient between the glass and ambient
hg_a = hg_a_rad + hw;
%overall the heat transfer coefficient between the glass and ambient
hf_p= 350; %heat transfer coefficients between fluid and absorber tube
Ust= 1/(0.1+t/ks+0.01); %heat transfer coefficient of storage tank
eff=0.8;
fw=2*eff-1;
Tc=(Tfi+Ti)/2;
```

```
% glass temperature in evacuated tube solar collector at tstep
Tg1= (tstep/cg)*(eg*s*(Tsky.^4-Tgi.^4)+ hg_a*(AT-Tgi) +
eg*s*(Tpi.^4-Tgi.^4))+ Tgi;
% absorber temperature in evacuated tube solar collector at tstep
Tp1= (tstep/cg)*(tg*ag*It+eg*s*(Tg1.^4-Tpi^4) + hf_p*(Tfi-Tpi))+
Tpi;
%fluid temperature in evacuated tube solar collector at tstep
Tf = (tstep/(m*cp))*((Ac*hf_p*(fw*Tp1-Tc))- mdot*cp*(Tfi-Ti))+Tfi;
%the instantaneous temperature of water exits from collector at tstep
%s1=1-(As*Ust*tstep/(m*cp));
%s2=0.2*(mdot*tstep/(m*cp));
%s3=As*Ust*tstep/(m*cp);
%Ts1=s1*Tf+s3*Tai+s2*Tfi;
Ts1=30;
Ts11 = Ts1;
end
end
```

%Main Program

```
for i=1:365
GRR=data1(:,1,i);
DRR=data1(:,2,i);
ATT=data1(:,3,i);
Tmilkin = 32;          % initial milk temperature
Tm =32;
Twr = Tmilkin+2;       % initial return water temperature
for j=1:24
GR=GRR(j);
```

3

```
DR=DRR(j);
AT=ATT(j);
%The ratio of beam radiation on the tilted surface
Rb=((cos(phiibeta))*cos(decl(i))*cos(omega(j))+sin(decl(i))*(sin(phii-
beta)))/(cos(phii)*cos(decl(i))*cos(omega(j))+(sin(decl(i))*sin(phii)));
It=Rb*(GR-DR)+(DR*0.5*(1+cos(beta)))+(0.5*Rf*((1-
cos(beta))*GR));
In=It*ag*tg;       % solar Energy on inclined surface
if In<0
In=0;
end
for jj=1:60
Tpo=(Tp1+Tpi)/2;
Tgo=(Tg1+Tgi)/2;
Tfo=(Tf+To)/2;
Tsky= AT-6;          %sky temperature of the selected site
hw=5.7+(3.8*Vw);     %convection heat transfer coefficient around the outer
glass tube
hp_g_rad1 = (eg-ep)*s*((Tpo.^4-Tgo.^4)/(Tpo-Tgo));
hg_a_rad1 = eg*s*(((Tgo).^4)-((Tsky).^4))./(Tgo-Tsky);
%radiation heat transfer coefficient between the glass and ambient
hg_a1 = hg_a_rad + hw;
hf_p= 350;
Tg= (tstep/cg)*(eg*s*(Tsky.^4-Tgo.^4)+ hg_a1*(AT-Tgo) +
eg*s*(Tpo.^4-Tgo.^4))+  Tgo;  %glass  temperature  in  evacuated  tube  solar
collector at tstep
if Tg<0
```

```
Tg=0;
end
Tp= (tstep/cg)*((tg*ag*It)+eg*s*(Tg.^4-Tpo.^4) + hf_p*(Tfo-
Tpo))+ Tpo; %absorber temperature in evacuated tube solar collector at tstep
Ust= 1/(0.1+t/ks+0.01); %heat transfer coefficient of storage tank
eff=0.8;
fw=2*eff-1;
Tc1=(Tfo+Ti)/2;
UL= 1/((1/hg_a_rad1+hw)+(1/hp_g_rad1)); %overall heat loss coefficient of the
tube
Qabs= ag*tg*It*Aabs; %total solar radiation absorbed by absorber plate
Qthermal_loss = (UL*Aig*(Tp-AT)); %heat lost by tubes
Qu = Qabs-Qthermal_loss; %useful energy output of evacuated tube solar collector
if Qu<0
Qu=0;
end
%The collector outlet water temperature at tstep
Tf1 =(tstep/(m*cp))*((Ac*hf_p*(fw*Tp-Tc1))-Qu)+Tfo;

%%%% Correlation Coefficients
Nui = 0.0397*((Re)^0.784)*((pr1)^0.3); % inner Nusselt number correlation
Ra = Gr*pr2;
Nuo = 0.36+((0.518*(Ra)^0.25)/(1+(0.559/pr2)^(9/16))^(4/9)); % outer Nusselt
number correlation
hi = (Nui*k1)/(2*ri);   % inner conv.
ho = (Nuo*k2)/(2*ro);    % outer conv.
U1 = 1/((ro/(ri*hi))+((ro/kc)*(log(ro/ri)))+(1/ho)); % overall heat transfer
coeffient
%%%%
Ams = 0.831;     %% % closed outer surface area of milk storage tank
ksm = 0.036;     %% % thermal conductivity of glass fiber, w/mk
tt  = 0.12;       %% % thickness of insulator
Usm =1/(0.01+t/ksm+0.01); %storage tank water temperature supplied to the next
loop
if ((j>8) &(j<18))
Qload= mdotw*cp*(Ts11-Twr);    % Rate of heating Load required
Qgain = mdot*cp*(Tf1-Ts11);   % rate of energy outlet from the collector
else
Qload =0;
Qgain=0;
end
Qloss = As*Ust*(Ts11-AT); % rate of energy lost from storage tank
Q11 =(Qgain -Qload- Qloss);
Ts11= Ts11+((tstep*Q11)/(mst*cp)); % water temperature inlet to the coil/ in
the storage tank
%%%%%%%%%%%%%%%%
Tlmtd = ((Ts11-Tm)-(Twr-Tmilkin))/(log((Ts11-Tm)/(Twr-Tmilkin))); % log mean
temperature difference
if Tlmtd <0;
Tlmtd =0;
end
Qlossm = tstep*Ams*Usm*(Tm-AT);        %heat loss from milk storage tank
Twr = Ts11-((U1*Ao*Tlmtd)/(mdotw*cp)); %return water temperature
if ((j>10)&(j<18))
Qloadf = Qload-Qlossm;
Tmilkin = Tm;
```

```
Tm = Tmilkin+(tstep*Qloadf)/(mm*cppm); %Temperature of milk pasteurized
Tmilk = Tm;
end
end
% useful heat, glass temperature, water temperature exits the collector, water
temperature in storage tank, Temperature of milk pasteurized and % coefficients
of performance for each day of the stored as;
Qum(i,j) = Qu;           % Useful energy
Tgm(i,j) = Tg;           % Glass temperature
Tfm(i,j) = Tf1;          % Collector exit water
Tsm(i,j) = Ts11;
Tppm(i,j)= Tm;
Int(i,j)=In;
Qgain1(i,j)=Qgain;
Tlmtd1(i,j)= Tlmtd;
Twr1(i,j)=Twr;
Tmilknn(i,j)= Tmilkin;
end
end
% plot Solar Radiation on inclined surface
jj=1:24;
InlJ17=Int(17,:);InlF16=Int(47,:);InlM16=Int(75,:);InlA15=Int(105,:);...
InlM15=Int(135,:);InlJ11=Int(162,:);InlJu17=Int(198,:);InlA16=Int(228,:);...
InlS15=Int(258,:);InlO15=Int(288,:);InlN14=Int(318,:);InlD10=Int(344,:);...
InlOct15=Int(288,:);
plot(jj,InlJ17,'k--',jj,InlF16,'b
x',jj,InlM16,'r*',jj,InlA15,'g-',jj,InlM15,'b--',...
jj,InlJ11,'k-d',jj,InlJu17,'r-*',jj,InlA16,'g-s',jj,InlS15,'kx',
jj,InlOct15,'b-*',...
jj,InlN14,'r-h',jj,InlD10,'g-*','linewidth',2);
xlabel(' Hour of day')
ylabel(' Solar irradiance (W/m^2)')
title('Monthly Average Solar Radiation on Inclined Surface ')
legend('January17','February16','March16','April15','May15','June11','July17'
,.....
'August16','September15','October15','November14','December10')
grid on
pause
clf
QumJ17=Qum(17,:);QumF16=Qum(47,:); QumM16=
Qum(75,:);QumA15=Qum(105,:); QumM15=Qum(135,:);
QumJ11=Qum(162,:);QumJu17=Qum(198,:); QumA16=Qum(228,:);
QumS15=Qum(258,:);QumOct15=Qum(288,:);QumN14=Qum(318,:);QumD10=Qum(344,:);
jj=1:24;
% Plots mean monthly useful heat arrived to absorber plate
plot(jj,QumJ17,'k-',jj,QumF16,'b-',jj,QumM16,'r-',jj,QumA15,'g-
',jj,QumM15,'b--',...
jj,QumJ11,'k--',jj,QumJu17,'r--',jj,QumA16,'g--',jj,QumS15,'k
x',jj,QumOct15,'b*',...
jj,QumN14,'r*',jj,QumD10,'g*','linewidth',2);
xlabel(' Hour of day')
ylabel(' Energy (W)')
title ('Monthly Average Hourly Useful Heat Gained ')
legend
('January17','February16','March16','April15','May15','June11','July17',.....
'August16','September15','October15','November14','December10')
```

```
grid on
pause
clf
% Plots mean monthly glass temperature
TabJ17=Tgm(17,:);TgmF16=Tgm(47,:);TabM16=
Tgm(75,:);TgmA15=Tgm(105,:);...
TgmM15=Tgm(135,:);TabJ11=Tgm(162,:);TgmJu17=Tgm(198,:);TgmA16=Tgm(228,:);...
TgmS15=Tgm(258,:);TgmOct15=Tgm(288,:);TgmN14=Tgm(318,:);TgmD10=Tgm(344,:);...
jj=1:24;
plot(jj,TabJ17,'k-',jj,TgmF16,'b-',jj,TabM16,'r-',jj,TgmA15,'g-
',jj,TgmM15,'b--',...
jj,TabJ11,'k--',jj,TgmJu17,'r--',jj,TgmA16,'g--',jj,TgmS15,'k
x',jj,TgmOct15,'b*',...
jj,TgmN14,'r*',jj,TgmD10,'g*','linewidth',2);
xlabel(' Hour of day')
ylabel(' Temperature (^0C) ')
title('Monthly Average Glass Temperature ')
legend('January17','February16','March16','April15','May15','June11','July17'
,.....
'August16','September15','October15','November14','December10')
grid on
pause
clf
% Plots mean monthly water temperature exit from the collector
TfmJ17=Tfm(17,:);TfmF16=Tfm(47,:);TfmM16=
Tfm(75,:);TfmA15=Tfm(105,:);...
TfmM15=Tfm(135,:);TfmJ11=Tfm(162,:);TfmJu17=Tfm(198,:);TfmA16=Tfm(228,:);...
TfmS15=Tfm(258,:);TfmOct15=Tfm(288,:);TfmN14=Tfm(318,:);TfmD10=Tfm(344,:);...
jj=1:24;
plot(jj,TfmJ17,'k-',jj,TfmF16,'b-',jj,TfmM16,'r-',jj,TfmA15,'g-
',jj,TfmM15,'b--',...
jj,TfmJ11,'k--',jj,TfmJu17,'r--',jj,TfmA16,'g--',jj,TfmS15,'k
x',jj,TfmOct15,'b*',...
jj,TfmN14,'r*',jj,TfmD10,'g*','linewidth',2);
xlabel(' Hour of day')
7
ylabel(' Temperature (^0C) ')
title('Monthly Average Water Temperature Exit from the Collector')
legend
('January17','February16','March16','April15','May15','June11','July17',.....
'August16','September15','October15','November14','December10')
grid on
pause
clf
% Plots mean monthly Temperature of water inlet to coil
TsmJ17=Tsm(17,:);TsmF16=Tsm(47,:);TsmM16=
Tsm(75,:);TsmA15=Tsm(105,:);...
TsmM15=Tsm(135,:);TsmJ11=Tsm(162,:);TsmJu17=Tsm(198,:);TsmA16=Tsm(228,:);...
TsmS15=Tsm(258,:);TsmOct15=Tsm(288,:);TsmN14=Tsm(318,:);TsmD10=Tsm(344,:);...
jj=1:24;
plot(jj,TsmJ17,'k-',jj,TsmF16,'b-',jj,TsmM16,'r-',jj,TsmA15,'g-
',jj,TsmM15,'b--',...
jj,TsmJ11,'k--',jj,TsmJu17,'r--',jj,TsmA16,'g--',jj,TsmS15,'kx',
jj,TsmOct15,'b*',...
jj,TsmN14,'r*',jj,TsmD10,'m -','linewidth',1);
xlabel(' Hour of day')
```

```
ylabel(' Temperature (^0C) ')
title('Monthly Average Thermal Storage Tank Water Temperature ')
legend('January17','February16','March16','April15','May15','June11','July17'
,.....
'August16','September15','October15','November14','December10')
grid on
pause
clf
% Plots mean monthly milk pasteurized;
TppmJ17=Tppm(17,:);TppmF16=Tppm(47,:);TppmM16=
Tppm(75,:);TppmA15=Tppm(105,:);...
TppmM15=Tppm(135,:);TppmJ11=Tppm(162,:);TppmJu17=Tppm(198,:);TppmA16=Tppm(228
,:);...
TppmS15=Tppm(258,:);TppmOct15=Tppm(288,:);TppmN14=Tppm(318,:);TppmD10=Tppm(34
4,:);...
jj=1:24;
plot(jj,TppmJ17,'k-',jj,TppmF16,'b-',jj,TppmM16,'r-',jj,TppmA15,'g-
',jj,TppmM15,'b--',...
jj,TppmJ11,'k--',jj,TppmJu17,'r--',jj,TppmA16,'g--',jj,TppmS15,'kx',
jj,TppmOct15,'b*',...
jj,TppmN14,'r*',jj,TppmD10,'m -','linewidth',1);
xlabel('Hour of day')
ylabel('Temperature (^0C)')
title('Monthly Average Pasteurized Milk Temperature')
legend('January17','February16','March16','April15','May15','June11','July17'
,.....
'August16','September15','October15','November14','December10')
grid on
xlim ([7 20])
pause
clf
```

Published with MATLAB® R2017a

Appendix C: Properties of Various Materials

Table C.1: Evacuated tube solar collector heat transfer coefficients

Coefficients	Value (W/m^2 K)	Source
$h_{r-g,rad}$	0.43	$h_{r-g,rad} = \frac{\sigma(T_r^2+T_g^2)(T_r+T_g)}{1/\varepsilon_r+1/\varepsilon_g-1}$
h_{r-g}	0.43	$h_{r-g} = h_{r-g,rad} + h_{r-g,cond}$
$h_{g-a,rad}$	0	Neglectable
$h_{g-a,conv}$	12.4	$h_{wind} = 5.7V + 3.8$
h_{g-a}	12.4	$h_{g-a} = h_{g-a,rad} + h_{g-a,conv}$
h_{r-a}	0.6	Experimental results
h_f	$h_f = \frac{\lambda_f}{D}Nu$	$Nu = 1.75\left[Gz + 5.6\times10^{-4}\left(Gr_f\ Pr_f\frac{L}{D}\right)^{0.70}\right]^{1/3}\left(\frac{V_{av}}{V_{wall}}\right)$

Continued

Coefficients	Value (W/m^2 K)	Source
$h_{r-Al,rad}$	0.35	$h_{r-\mathrm{Al},rad} = \frac{\sigma(T_r^2+T_{\mathrm{Al}}^2)(T_r+T_{\mathrm{Al}})}{1/\varepsilon_r+1/\varepsilon_{\mathrm{Al}}-1}$
$h_{r-Al,cond}$	26.7	$h_{r-\mathrm{Al},cond} = \lambda_{air1}/\delta_{air1}$
$h_{r-\mathrm{Al}}$	27.05	$h_{r-\mathrm{Al}} = h_{r-\mathrm{Al},rad} + h_{r-\mathrm{Al},cond}$
$h_{\mathrm{Al-Cu},rad}$	0.58	$h_{\mathrm{Al-Cu},rad} = \frac{\sigma(T_{\mathrm{Al}}^2+T_{\mathrm{Cu}}^2)(T_{\mathrm{Al}}+T_{\mathrm{Cu}})}{1/\varepsilon_{\mathrm{Al}}+1/\varepsilon_{\mathrm{Cu}}-1}$
$h_{\mathrm{Al-Cu},cond}$	26.7	$h_{r-\mathrm{Al},cond} = \lambda_{air2}/\delta_{air2}$
$h_{\mathrm{Al-Cu}}$	27.28	$h_{\mathrm{Al-Cu}} = h_{\mathrm{Al\text{-}Cu},rad} + h_{\mathrm{Al-Cu},cond}$

Table C.2: Physical properties of manifold header construction materials

Parameter	Symbol	Value	Unit
Material of internal cover of the manifold header (Stainless steel cover)			
Thermal conductivity of the internal cover	K_1	15	W/m k
Thickness of internal cover	e_1	1.2	mm
Insulating material (Polyurethane foam)			
Thermal conductivity of Insulating material	K_2	0.06	W/m k
Thickness of Insulating material	e_2	15	mm
Material of internal cover (Stainless steel)			
Thermal conductivity of the internal cover	K_3	15	W/m k
Thickness of internal cover	e_3	1.2	mm

Table C.3: Properties of Insulation Materials

Materials	**Density, ρ Kg/m^3**	**Thermal Conductivity, W/m.K**
Glass fiber	56–72	0.032–0.039
Polyurethane foam	24–40	0.023–0.026
Foamed Glass	144	0.058
Calcium Silicate	240	0.54
Phenolic Foam	35-120	0.018 - 0.022
Polystyrene Foam	30 -60	0.033 -0.045
polystyrene	15 -30	0.033 -0.038

Appendix D-1: Moody Chart

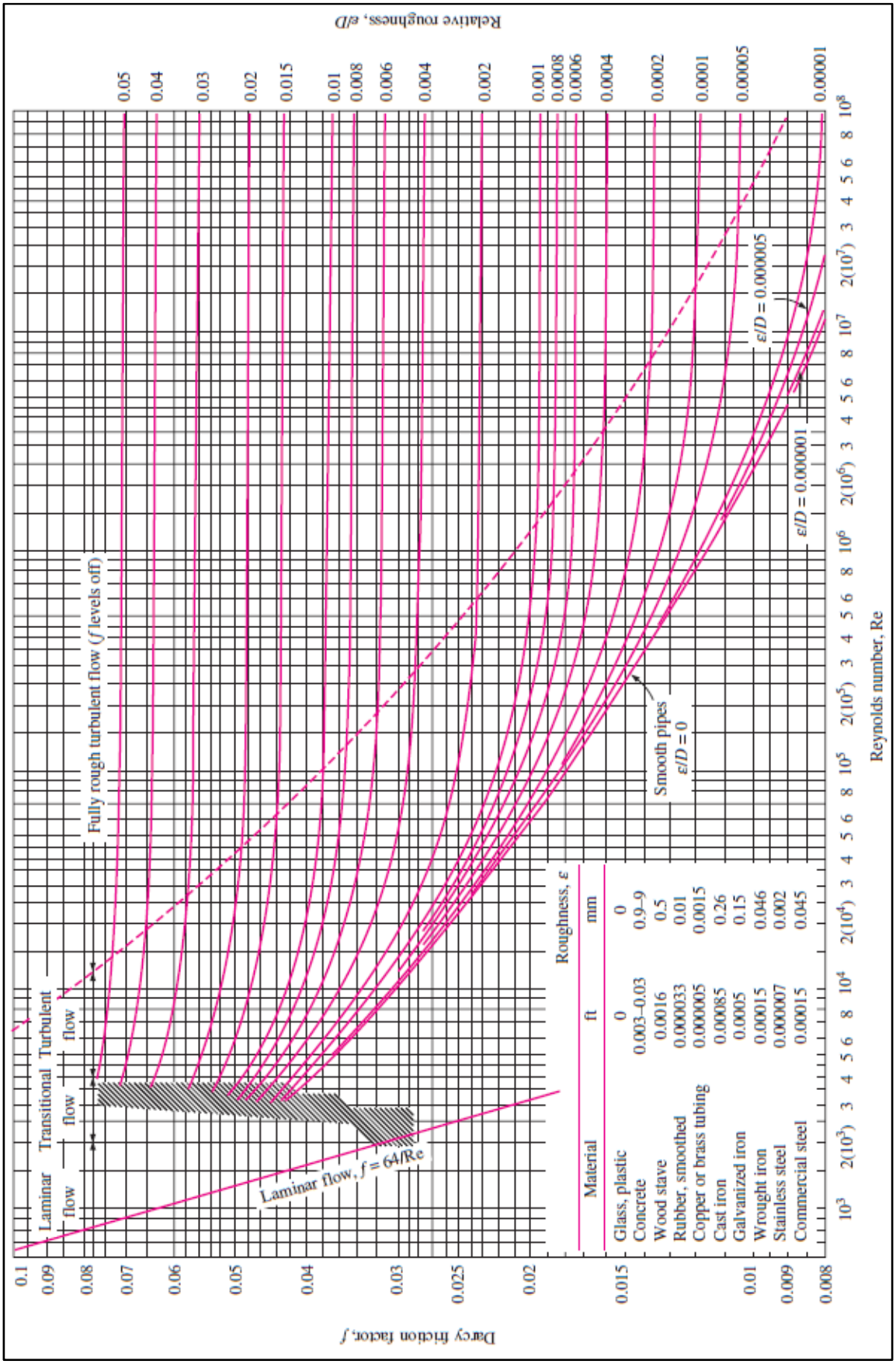

Figure D.1: Moody Chart

Appendix D-2: Economic Thickness of Insulation

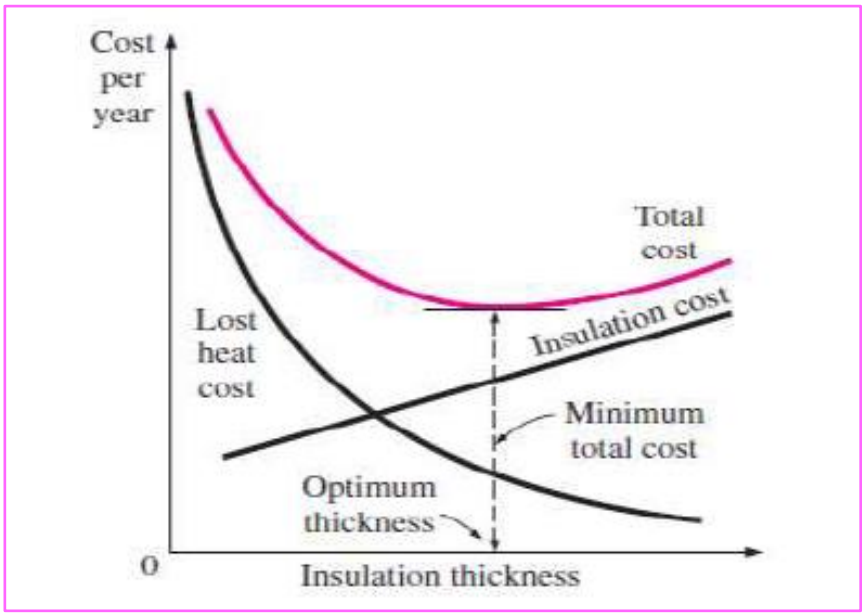

Figure D.2: Determination of the optimum thickness of insulation

Appendix D-3: Solar Water Pump Selection Chart

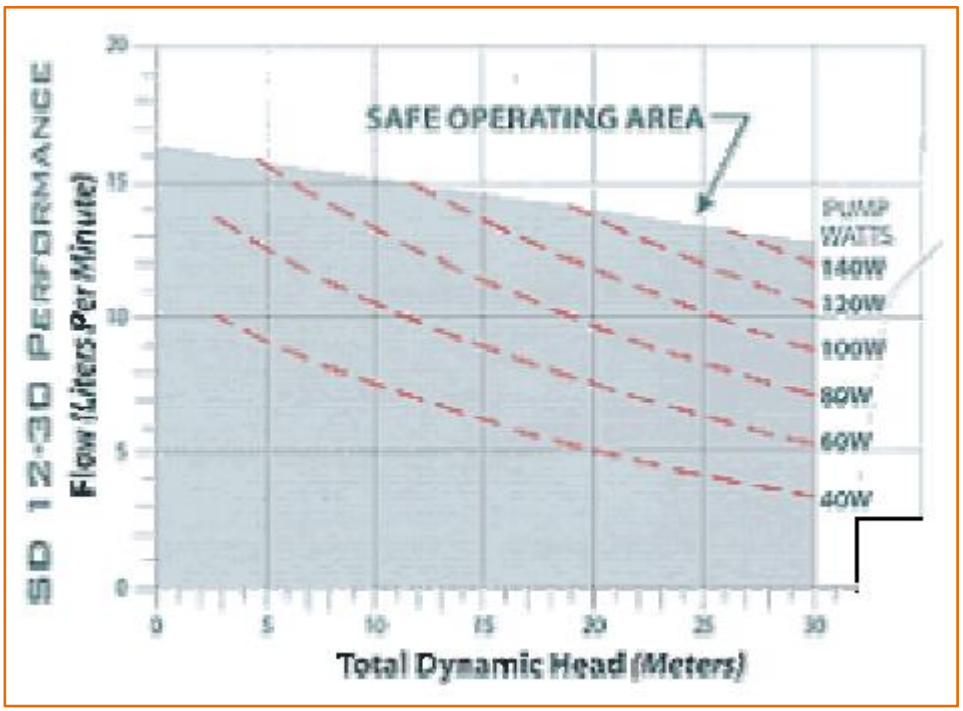

Figure D.3: A graph used to size a pump (from Kyocera Solar)